INFORMATION TO USERS

This manuscript has been reproduced from the microfilm master. UMI films the text directly from the original or copy submitted. Thus, some thesis and dissertation copies are in typewriter face, while others may be from any type of computer printer.

The quality of this reproduction is dependent upon the quality of the copy submitted. Broken or indistinct print, colored or poor quality illustrations and photographs, print bleedthrough, substandard margins, and improper alignment can adversely affect reproduction.

In the unlikely event that the author did not send UMI a complete manuscript and there are missing pages, these will be noted. Also, if unauthorized copyright material had to be removed, a note will indicate the deletion.

Oversize materials (e.g., maps, drawings, charts) are reproduced by sectioning the original, beginning at the upper left-hand corner and continuing from left to right in equal sections with small overlaps.

Photographs included in the original manuscript have been reproduced xerographically in this copy. Higher quality 6" x 9" black and white photographic prints are available for any photographs or illustrations appearing in this copy for an additional charge. Contact UMI directly to order.

ProQuest Information and Learning
300 North Zeeb Road, Ann Arbor, MI 48106-1346 USA
800-521-0600

UMI®

Infrared Spectroscopic Studies of the Main Cellular Components. The Effect of Hydration on Proteins, Nucleic Acids and Phospholipids Spectra

by

Alex Pevsner

A dissertation submitted to the Graduate Faculty in Chemistry in partial fulfillment of the requirement for the degree of Doctor of Philosophy, The Graduate School and University Center of City University of New York.

2002

ProQuest Information and Learning Company
300 North Zeeb Road
P.O. Box 1346
Ann Arbor, MI 48106-1346

This manuscript has been read and accepted for the Graduate Faculty in Chemistry in satisfaction of the dissertation requirements for the degree of Doctor of Philosophy.

12/11/2001

Date

Chair of Supervisory Committee

12/11/2001

Date

Executive Officer

Professor John Lombardi

Professor Lou Massa

Doctor Luis Chiriboga

Supervisory Committee

The City University of New York

Abstract

Infrared Spectroscopic Studies of the Main Cellular Components. The Effects of Hydration on Protein, Nucleic Acid and Phospholipid Spectra.

by Alex Pevsner

Adviser: Professor Max. Diem

The research presented in the thesis was undertaken to examine effect of hydration of infrared spectra of the major cellular components: proteins, nucleic acids and phospholipids. A method was devised that utilizes KBr pellets to determine infrared bands of these biomolecules that are most sensitive to the variation in amount of bound water in the structure of these biomolecules. For proteins, an enormous increase in the absorption intensities of the amide I and amide II vibrations between dry and hydrated phases was observed. The intensity changes between dry and hydrated protein samples were interpreted in terms of variations in the dielectric constant of the immediate surroundings of a peptide linkage.

For nucleic acids, DNA and RNA, as well as phospholipids the symmetric and antisymmetric stretching vibrations of phosphate linkage, PO_2^-, were found to be very sensitive to hydration, as both intensity changes as well as frequency shifts are observed. The frequency shifts were interpreted in terms of the conformational changes, whereas the increase in intensity may be due to an increase in a local dielectric in the vicinity of the polar and solvent exposed phosphate groups.

Dedicated to my Family

My grandfather Zelik, my father Jacob, my mother Tamara and my brother Edgar who taught me the importance of education and settle for nothing but the best

Acknowledgments

First and foremost I would like to thank my research adviser Prof. Max Diem for his supervision and guidance. My laboratory partners Dr. Peter Lasch and Anthony Pacifico for their advice and assistance with my experiments. I also would like to thank the great teachers I had, Dr. Bernard Eisenberg, Dr. John Lombardi and Dr.Lou Massa, and all other who help me to achieve my goals.

Table of Content

List of Figures

Chapter 4: Hydration of Protein, Nucleic Acid and Phospholipid Films

Chapter 5: Attenuated Total Reflection (ATR) and Comparison of ATR and Transmission Measurements

Introduction

During the past decade, infrared spectra of human cells and tissue have been reported by a number of research groups. Although the routine studies of cells by infrared spectroscopy have started not so long ago, the pace of progress in this field in has been very impressive. Infrared spectroscopy has been shown to have the ability to differentiate between normal and cancerous cells[1-3], different cell types [4-7], stages of differentiation, maturation[8] and cell cycle phases [9]. The most recent advance in this field was the collection of an infrared map of a single cell with a spatial resolution of 6 μm via infrared microscope coupled to a synchrotron source [10]. The motivation for using spectroscopic techniques to assess cells and tissues is the fact that these methods detect chemical composition, and compositional changes of cells and tissue caused by a variety of conditions and diseases. Standard pathological methods, on the other hand, detect variations in morphology, tissue architecture, staining patterns, or sensitivity to a number of specific stains. However, although these methods are well-established, they require extensive sample preparation, and ultimately, a trained pathologist to interpret the microscopic images. Thus, pathological diagnosis is subjective.

Spectroscopic methods can be implemented such that they are completely objective, since spectral data, which are related to the composition of the sample, can be collected and interpreted by computer-based algorithms. However, for such computer-based methods to succeed, a detailed understanding of vibrational spectra of main cellular components is required. Besides band

assignments, the variations of infrared spectra with experimental conditions must be investigated in order to construct spectral database that is both accurate and free of artifacts due to variations in sampling conditions.

The work presented in this thesis addresses one of the particular artifacts that may be encountered when cells or sections of tissue are dehydrated by treatment with fixatives, such as ethanol, or by air-drying prior to collection of an infrared data. The purpose of such treatment is to remove water from cells. This prevents samples from degradation by bacteria, and also preserves cells and tissues for the use in a future experiments. However, removing water that is tightly bound in the structure of proteins, nucleic acids and phospholipids effects their molecular structure and conformation, and consequently, the infrared patterns observe for these biomolecules. Thus, dehydration conditions have a direct influence on the appearance of the spectra observed for proteins and nucleic acids and phospholipids . Understanding the effect of hydration on the vibrational spectra of the main cellular components is essential for the proper interpretation of spectra of cells and tissues, as well as to the development of consistent and artifact-free IR sampling procedure.

Infrared Spectra of the Main Cellular Components and Cells.

Typical infrared spectra of human cells are shown in Figure 1. The spectrum shown in this figure is that of a typical epithelial (mucosa) cell which was air dried on BaF_2 window . The most intense bands are those of proteins observed at *ca.*1655 and 1540 cm^{-1}. The lower frequency region of the cell

spectrum from 900 cm^{-1} to about 1300 cm^{-1} is dominated by PO_2^- vibrations of nucleic acids, DNA and RNA, and phospholipids . Another characteristic phospholipid peak is often seen as weak shoulder at *ca.* 1735 cm^{-1}. The infrared spectrum of a cell can be roughly approximated as a sum of the protein, nucleic acids and phospholipid spectra. This is a valid assumption, as protein compose about 60% of dry cell by mass, nucleic acids 25 % , and the rest of contributions coming from phospholipid and other compounds that are present in a cell [11].

Infrared spectra of major cellular components are shown on Figure 2. The distinct features of a protein spectrum are intense peaks around 1650 cm^{-1} , 1540 cm^{-1} and around 1300 cm^{-1}. These protein bands are known as amide I, II and III, and are due to a various vibrations of peptide linkage. The characteristic attributes of infrared spectrum of nucleic acid are the PO_2^- symmetric stretching mode observe at ca. 1090 cm^{-1} and antisymmetric stretching mode of the same moiety seen at around 1240 cm^{-1} . The contribution from double bonds vibrations, C=O, C=N and C=C, of amine bases to the spectrum of nucleic acid comes in the form of a broad band around 1650 cm^{-1}. Because of the presence of PO_2^- group, phospholipids as well as nucleic acids have bands at ca. 1090 cm^{-1} and ca. 1240 cm^{-1} which are ν_S PO_2^- and ν_{AS} PO_2^- . Yet, phospholipids have features that are specific only to this class of biomolecules, namely the CH_2 rocking mode observed at 1469 cm^{-1} and the C=O stretching vibration seen at *ca.* 1740 cm^{-1}. A more detailed analysis of vibrational modes of the main cellular components as well as their response to the hydration will be discuss in a subsequent chapters.

Reference

1. Wong, P,T.; Wong, R,K.; Caputo, T,A.; Godwin,T,A.; Rigas, B. IR Spectroscopy of Exfoliated Human Cervical Cells; Evidence of Extensive Structural Changes During Carcinogenesis. *Proc. Natl.Acad.Sci.USA.* **1991,** 88,10988-10992.

2. Cohenford, M.; Rigas ,B. . Cytologically normal cells from neoplastic cervical samples display extensive structural abnormalities on IR spectroscopy: Implications for tumor biology. *Proc. Natl. Acad.Sce.USA.* **1998**, 95, 15327-15332.

3. Benedetti, E.; Bramanti, E.; Papineschi,F.; Rossi,I.;Benedetti,E. Determination of the Relative Amount of Nucleic Acids and Proteins in Leukemic and Normal Lymphocytes by Means of Fourier Transform Infrared Microspectroscopy (FT-IR-M). *Appl.Spectrosc.* **1997**, 51 (6),792-797.

3. Nauman,D.; Fijala,V.; Labischinski,H.; .Giesbrecht, P. The rapid differentiation and identification of pathogenic bacteria using FT-IR and multivariate statistical methods. *J.Mol. Struct.* **1988**, 174, 165-170.

4. Helm,D.; Labischinski,H.; Schallen, G.; Naumann, D. Classification and identification of bacteria by FT-IR spectroscopy. *J.Clin.Microbiol.* **1991**,137, 69-79.

5. Sockaland, S,G.; Bouhedja,W.; Pina, P.; Allouch, P.; Bloy,C.; M.Monfait,M. FT-IR Spectroscopy as an Emerging Method for Rapid Characterization of Microorganisms. *Cell.Mol. Biol.* **1998**, 44 (1), 261-269.

7. Ngo-Thi,N,A.; Kirschner,C.; Naumann,D.; FT-IR mircoscopy: a rapid method for classifying microorganisms. In *Spectroscopy of Biological Molecules: New Directions;* Greve, J.,Puppels G.J,. Otto, C.,Eds.; Kluwer Academic Publishers: Dordrecht (Netherlands),1999: pp.557-559.

8. Chiriboga,L.; Xie,P.; Yee,H.;Vigorita,V.; Zarou.D.; Zakim,D.; Diem,M. Infrared Spectroscopy of Human Tissue: I. Differentiation and Maturation of Epithelial Cells in the Human Cervix. *Biospectrosc,***1998**,4, 47–54.

9. Boydston-White,S.; Gopen,T.; Houser,S.; Bargonetti,J.; Diem,M. Infrared Spectroscopy of Human Tissue: V. Infrared spectroscopic studies of Myeloid Leukemia (ML-1) cells at different phases of the cell cycle. *Biospectrosc*, **1999**, **5**, 219-227.

10. Lasch, P.; Pacifico, A.; Chiriboga, L.; Diem, M. Infrared Microspectroscopy and Infrared Spectral Maps of Single Human Cells. *Nature*, submitted for publication 2001.

11. Diem, M.; Boydston-White, S.; Chiriboga, L.; Infrared spectroscopy of Cells and Tissues: Shining Light onto a Novel subject. *Appl.Spectrosc.***1999**, 53 (4),148A-161A.

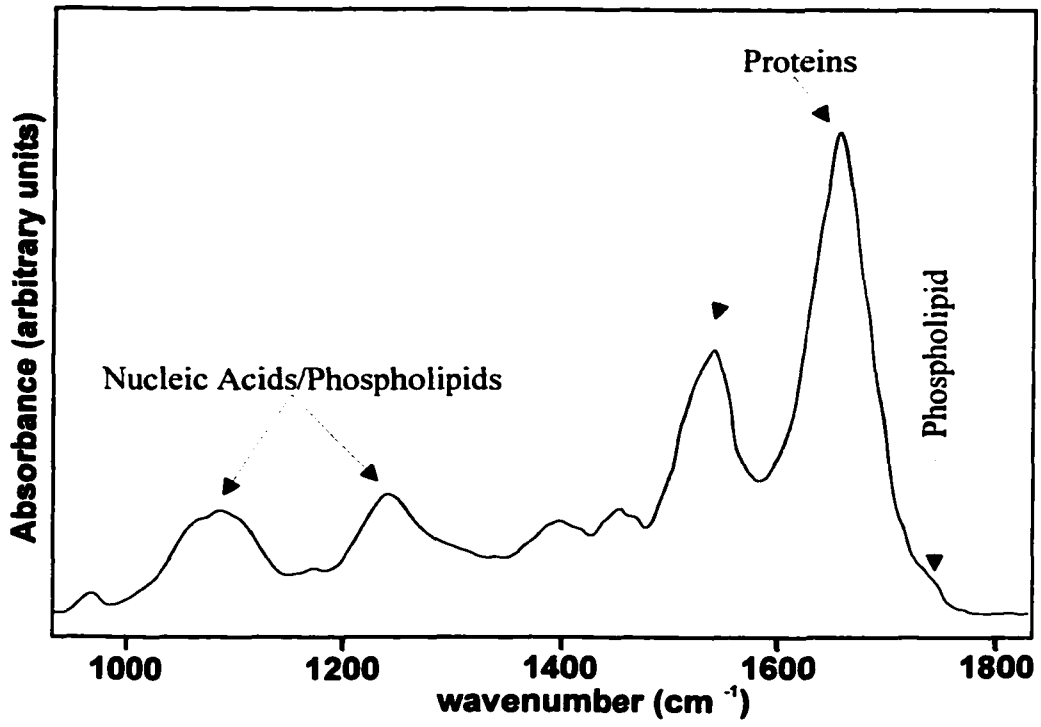

Figure 1. FT-IR absorption spectrum of epithelial cells.

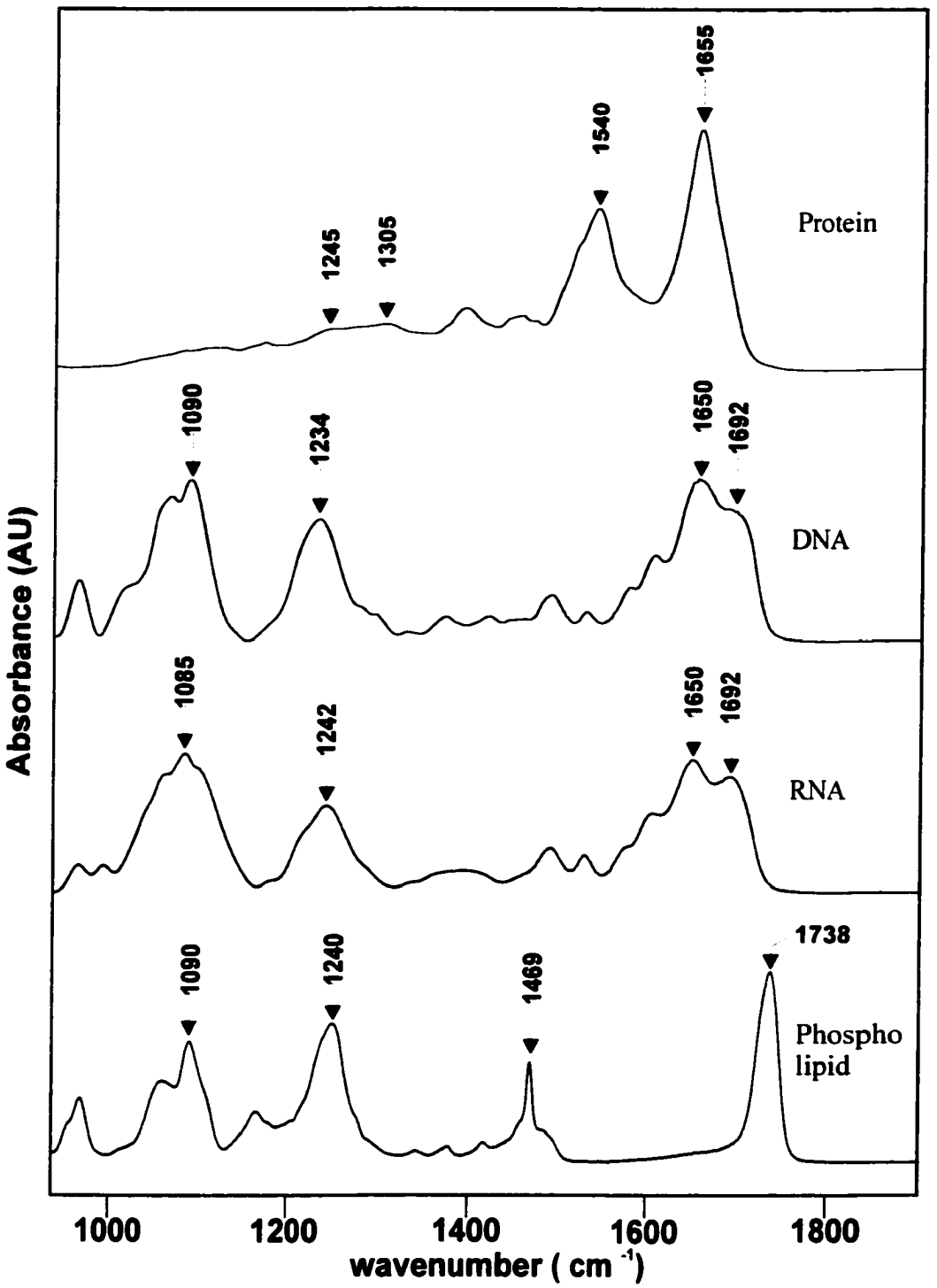

Figure 2. FT-IR absorption spectra of the main cellular components: protein, DNA, RNA and phospholipid.

Chapter 1: Theory and Practice of Infrared Spectroscopy

Infrared spectroscopy is a technique that enables the observation of vibrational transitions in a molecule. Infrared refers to a region of the electromagnetic spectrum that covers a wavelengths range from 5×10^{-3} to 2.5×10^{-4} cm or in wavenumber units from 4000-200 cm^{-1}. The energy of infrared photon can be computed from Einstein equation

$$E=hc\bar{\nu}$$

where **h** is a Planck's constant, **c** is a speed of light and $\bar{\nu}$ is wavenumber. The energy of infrared photon is about 2×10^{-20} Joules, and it can induce a vibrational transitions in a molecule. Infrared radiation was discovered by Sir William Hershel in 1800 in a set of experiments with sun light. He found that a thermometer placed beyond the red region of a solar spectrum was heated more than in a visible portion. A new form of radiation "infrared" was discovered. Infrared absorption studies of molecules began in early 1900s, and today infrared spectroscopy is one of the more popular and widely used spectroscopic methods. The strength of IR spectroscopy as an analytical technique lies in its ability to differentiate between vibrations of various functional groups, and the sensitivity of IR enables to detect even a minute changes in chemical environment of a particular bond or functional group. This particular feature of IR appeals most to biophysicists and biochemists, who utilize IR for structural

studies of proteins, nucleic acids, phospholipids and even more complex biological systems such as cells.

The infrared spectroscopic experiment consists of two parts a) collection of the spectrum and b) interpretation. To collect high quality spectra it is essential to know the inner working of modern infrared spectrometer. To interpret spectra, the thorough knowledge of the theory of infrared spectroscopy is an absolute prerequisite.

The instrumentation for collecting infrared data has improved dramatically over a past few decades. The major technological step in the construction of IR spectrometers was the switch from dispersive to Fourier Transform (FT) instruments. Personal computer and semiconductor technology played a key role in making an IR spectrometer what it is today. With modern FTIR spectrometer it is possible to collect data on a smaller amounts of sample, and the data acquisition time for a single spectrum is less than a minute. However, the theory of IR on the other hand has not changed since the classical work on vibrational spectroscopy by Wilson, Decius and Cross written in 1950's.

Theory.

1.1 Normal Modes of Vibration

The most important theoretical concept in vibrational spectroscopy is the concept of normal modes. Normal mode analysis (NMA) describes the complex vibrations of a molecule as a combination of simpler motions of individual atoms in a molecule. When calculated, normal modes describe a) what bonds or group

of atoms in molecules undergo vibrations and b) the frequency of those vibrations.

Normal mode analysis assumes that atoms are point masses that are held together by a spring that obeys Hook's law ,**Force = -kx**, hence NMA is a purely classical treatment of the vibrations of polyatomic molecule (Figure 1). Perhaps in explaining normal modes it is best to start with a description of a one-dimensional , one-particle system and then move on to the analysis of polyatomic molecule (Figure 2). The calculation starts with Newton's second law

$$\textbf{Force} = ma = -kx \qquad \textbf{eq.1}$$

$$ma + kx = 0 \qquad \textbf{eq.2}$$

The **Force** that a body experiences during a motion is given by a mass **m** times acceleration **a**, or a spring constant **k** times **x**, the displacement of the body from the its equilibrium position along the x- axis. The expression for **Force** can also be formulated in terms of both potential and kinetic energies of a moving particle. The potential energy of a simple harmonic oscillator is given by

$$V = 1/2kx^2 \qquad \textbf{eq.3}$$

Force is the first derivative of a potential energy with respect to a displacement

$$\textbf{Force} = -dV/dx = -kx \qquad \textbf{eq.4}$$

and a force constant **k** can be expressed as a second derivative of the potential energy

$$k = d^2V/dx^2 \qquad \textbf{eq.5}$$

The kinetic energy of a body is a function of mass and velocity

$$T = 1/2\ mv^2 \qquad \textbf{eq.6}$$

$$ma=d^2T/dt^2 \qquad \text{eq.7}$$

Eq.2 after substitutions becomes

$$d^2T/dt^2 + dV/dx=0 \qquad \text{eq.8}$$

In classical mechanics this equation is known as the **Lagrange** equation. However in a more familiar way eq.2 is written as

$$m\, d^2x/dt^2 + kx = 0 \qquad \text{eq.9}$$

This is second order differential equation, and it describes the motion of a mass under restoring force exerted by a spring. The solution to eq.9 is

$$x= A \sin (k^{1/2} t + b)$$

where **A** and **b** are integration constants.

For a molecule **3N** simultaneous equations have to be solved to describe a motion of each nuclei in a molecule. **N** is the number of atoms in a molecule multiply by 3 degrees of freedom, since individual atom can move in **x**, **y** and **z** direction. To simplify the calculation mass- weighted Cartesian coordinates are introduced, $q_i = \sqrt{m}x$. This term is a displacement of the ***i*th** nuclei from the equilibrium position.

For a molecule Newton's second law becomes

$$d^2q_i/dt^2 + \partial V/\partial q_i=0 \quad i=1.....,3N \qquad \text{eq.10}$$

The potential energy in eq.10 can shown to be

$$\partial V/\partial q_i = \sum_{j=1}^{3N} f_{ij}\, q_i q_j \qquad \text{eq.11}$$

and eq.10 becomes

$$d^2q_i/dt^2 + \sum_{j=1}^{3N} f_{ij}\, q_i q_j =0 \qquad \text{eq.12}$$

f_{ij} is force constant of a spring that holds two nuclei together, q_i and q_j are the displacements of two interacting atoms from there equilibrium positions. The term $\sum_{j=1}^{3N} f_{ij} q_i q_j$ has a direct physical meaning. It describes the interaction of one atom with every other atom in a molecule or the incremental energy the system experiences when the atom is moved along x,y or z direction. Eq.12 is a system of 3N simultaneous equations with 3N unknowns q_i .

In this from eq.12 can not be solved easily, because the potential energy term contains a product of two different coordinates that can not be separated. It is therefore desirable to have a potential energy term that is a function of only one coordinate. At this stage the normal coordinates Q_i are introduced. A *Normal coordinate* is a linear combination of the mass-weighted Cartesian coordinates. To obtain normal coordinates, an orthogonal similarity transform on the matrix **F** (with matrix elements that are force constant f_{ij}) is performed

$$FL=L\Lambda \qquad \text{eq.13}$$

$$L^{-1}FL=\Lambda \qquad \text{eq.14}$$

L is an orthogonal matrix that diagonalizes the force constant matrix **F** in to Λ. The columns of matrix **L** are eigennvectors of **F**, and Λ is diagonal matrix with eigenvalues λ_i. The coefficients of the columns of matrix **L** ,or eigenvectors of a force constant matrix **F**, provide the transformation from the Cartesian coordinates to normal coordiantes. The eigenvalues λ_i are related to the

frequencies of normal coordinates. In matrix notation the expression for a normal coordinate **Q** is ,

$$Q_i = \sum_{k=1}^{3N} l_{ik} q_k, \qquad \text{eq.15}$$

where l_{ik} are the matrix elements of matrix **L**

$$Q = L^{-1} q \qquad \text{eq.16}$$

Written in terms of normal coordinates eq.12 becomes

$$d^2Q_i/dt^2 + \sum_{j=1}^{3N} \lambda_i Q_i = 0 \qquad \text{eq.17}$$

Potential energy is now a function of only one coordinate and eq.12 can be solved to yield

$$Q_i = B_i (\sin (\lambda_n^{1/2} t + b_k) \qquad \text{eq.18}$$

This derivation shows that all atoms in a normal coordinate vibrate a) in phase and b) with the same frequency. The frequencies of normal modes can be shown to relate to eigenvalues of a force constant matrix by

$$\nu_i = \lambda_i^{1/2} / 2\pi \qquad \text{eq.19}$$

1.2 Intensity of normal mode vibration

Normal mode analysis allows the visualization of vibrations, yet it does not explain intensities of vibrational transitions nor does it explain whether a given vibrational mode is infrared active. For a vibrational transition to be infrared active a quantum mechanical selection rule must be satisfied, namely the transition must result in a change in the dipole moment of a molecule.

$$\mu_{\text{transition dipole moment}} = \langle \psi_0 | \mu | \psi_1 \rangle \qquad \text{eq.20}$$

In this equation ψ_o is a ground state vibrational wavefunction and ψ_1 is excited state function. μ is a dipole moment operator. The vibrational wavefuction can be computed by substituting the normal coordinate into the vibrational *Schrödinger* equation.

$$-\hbar/2\pi\, d^2\Psi_i/dQ_i^2 + \tfrac{1}{2}\,\Lambda_i Q_i^2 \Psi_i = E_i\Psi_i \qquad \text{eq.21}$$

Once the wavefuctions are known the transition dipole moment can be evaluated. The transition dipole moment corresponds to an observable **D**, the transition dipole strengths, which can be determined experimentally by integrating the area under the infrared band, graphed in molar absorptivity ε versus $\bar{\nu}$,wavenumer units.

$$D = \int(\varepsilon/\bar{\nu})\, d\bar{\nu} = |\langle\psi_0|\mu|\psi_1\rangle|^2 \qquad \text{eq.22}$$

Therefore, the greater the change in transition dipole moment produced by vibration the greater will be the integrated intensity of the band.

1.3 Calculation of vibrational spectra

There are number of software packages available, such as Gaussian® or Hyperchem®, that are able to calculate the vibrational spectrum of a molecule at different levels of theory , semi-empirical or *ab initio*. This is a particularly useful tool that is available to spectroscopists, because it makes possible to compare experimental results with theoretical and vices versa.

The calculation of a vibrational spectrum starts with optimizing a geometry of a molecule. Geometry optimization seeks to find a conformation of a molecule with lowest energy, and also ensures that there are no forces acting on the

atoms. Once geometry optimized, the *Hessian* or *force constant* matrix is computed. Force constant matrix contains the second derivatives of the total energy of a molecule with respect to the displacement of each atom in the x, y, and z direction. For a three-atom molecule (Figure 1) the Hessian matrix is computed as follows. Atom number 1 is chosen and is it moved by a small distance along the x-axis. When the atom is displaced form its equilibrium position the molecule will have new energy. The energy of a new conformation is recomputed and the second derivative with respect to a motion of the atom 1 in x direction is evaluated. This value then becomes a first element in the force constant matrix and it represents a restoring force that acts on the atom number 1 when it moves along x- axis. The atom 1 is then moved along y and z direction to calculate the force constants along these axes. The procedure is then repeated for atoms two and three, and a matrix with 9 by 9 or 3N by 3N elements is obtained. The force constant matrix is then diagonalized to solve for normal coordinates and frequencies of vibrations. A computational programs such as Hyperchem can also display vibrational spectrum and animate vibrations. The calculation of a vibrations spectrum is a particularly time consuming task and therefore even most sophisticated calculations are limited to molecules with only 20 to 30 atoms.

1.4 Instrumentation

The heart of modern infrared spectrometer is a device called an interferometer (Figure 3). The theory behind this device relies on the principle of

constructive and destructive interference of light waves. An interferometer has a beam splitter and two mirrors, a stationary and a movable one. Monochromatic wave travels from a source to a beam splitter where it is deflected in two directions, toward the stationary and the movable mirror. Two beams are then reflected by the mirrors and recombined at a beam splitter that directs the wave toward a detector that registers intensity of incoming radiation. Depending on the position of the movable mirror, the two beams will combine at the beam splitter constructively or destructively. Constructive interference will occur if distance traveled by the mirror,δ, is equal to

$$\delta=n\lambda \qquad n=0,1,2,3 \ldots$$

here λ is wavelength of light, and destructive interference,

$$\delta=n\ ½\ \lambda \qquad n=0,1,2,3 \ldots$$

Thus, from examining pattern of bright and dark spots or fringes at the detector, it is possible to determine the exact wavelength of monochromatic light. In fact, the interferometer was used by it is inventor Albert Michelson to measure accurately the wavelengths of light. For his invention and experimental work Michelson was awarded in 1907 the Nobel Prize in Physics and was the first American scientist to be given this prestigious award.

A monochromatic source can be substituted with a polychromatic source and a number of different wavelengths can be examined simultaneously. When a sample is placed in the path of the beam the wavelengths of light absorbed by a sample can be determined. The results of the measurement come in the form of a plot of intensity vs. distance traveled by the movable mirror or *interferogram*.

In this form the results can not be interpreted and therefore a Fourier transformation is performed. This mathematical procedure transforms the intensity from a function of mirror position to a function of a frequency of light.

$$I(\delta)= 1/\sqrt{2\pi} \int_{-\infty}^{+\infty} I(\nu)\, e^{i\delta\nu}\, d\nu \qquad \text{eq.23}$$

$$I(\nu)= 1/\sqrt{2\pi} \int_{-\infty}^{+\infty} I(\delta)\, e^{-i\delta\nu}\, d\delta$$

The interferogram is transformed to a new plot, intensity vs. frequency or *spectrum*, a conventional way of presenting the data of spectroscopic measurements (Figure 4). The use of mathematical transformation gives this spectroscopic technique its name Fourier Transform Infrared Spectroscopy or FT–IR.

Interferometers come in number of different designs, however all of them operate on the same principal. The Bruker Vector 22 and Vector 28 IF/S FT-IR spectrometers, which were used for most of the experimental work, presented in this thesis are of ROCKSOLID™ design developed by Bruker Optics. The source for Vector series instruments is globar, which is SiC or Nichrome wire heated between 1600-2400 K. Both spectrometers are also equipped with DGTS detectors (deuterated glycine sulfate) also know as a pyroelectric bolometer. This detector senses temperature changes which translate into voltage variations across the detector element. DGTS is a good choice for infrared routine measurements as it is inexpensive, robust and has good sensitivity over a large wavenumber range. The more expensive models such as Vector 28 IF/S have DGTS and MCT detectors. MCT (mercury cadmium telluride) is a semiconductor

detector. Infrared photons promote electrons from a valence band to a conducting band and create electric current the magnitude of which is proportional to intensity of infrared photons. MCT is about 5 times more sensitive then DTGS detector and also faster. However, MCT requires cooling with liquid nitrogen. The MCT is ideal when working with small amounts of a sample or with aqueous solutions. The subsequent data processing is done on the software provided by a manufacturer or using programs developed in the laboratory. The programs created "in house" generally tailored better to the needs of the laboratory. All software packages provide a similar set of common function for manipulating the spectra such as baseline correction, smoothing, differentiation, integration, curve fitting and etc. A more detailed analysis of instrumental and theoretical aspects of FTIR can be found in the literature that is cited in the reference section.

References

1. Wilson B.E; Decius,J,C; Cross, P.C. *Molecular Vibrations: The Theory of Infrared and Raman Vibrational Spectra*. McGraw-Hill: , New York, 1955.

2. Levine,Ira. *Molecular Spectroscopy*. John Wiley & Sons: New York, 1975.

3. Diem, Max. *Introduction to Modern Vibrational Spectroscopy*. John Wiley & Sons: New York, 1993.

4. Colthup,N,B;Daly,L,H; Wiberley,S,E. *Introduction to Infrared and Raman Spectroscopy*. 3rd Ed; Academic Press: New York,1990.

5. Foresman,J,B; Frish,E. *Exploring Chemistry with Electronic Structure Methods*. 2nd Ed; Gaussian, Inc: Pittsburgh, 1996.

6. Gaffey,M,L;Dobosh,P,A;Richardson,D,M. *Laboratory Exercises Using Hyperchem®*. Hypercube,Inc: Gainesville, Florida, 1998.

7. Griffiths, P,R; de Haseth, J,A. *Fourier Transform Infrared Spectroscopy*; Chemical Analysis; Vol 83. Jonh Wiley & Sons: New York,1986.

8. Smith,B,C. Fundamentals of Fourier Transform Infrared Spectroscopy. CRC Press: Boca Raton, Florida, 1995.

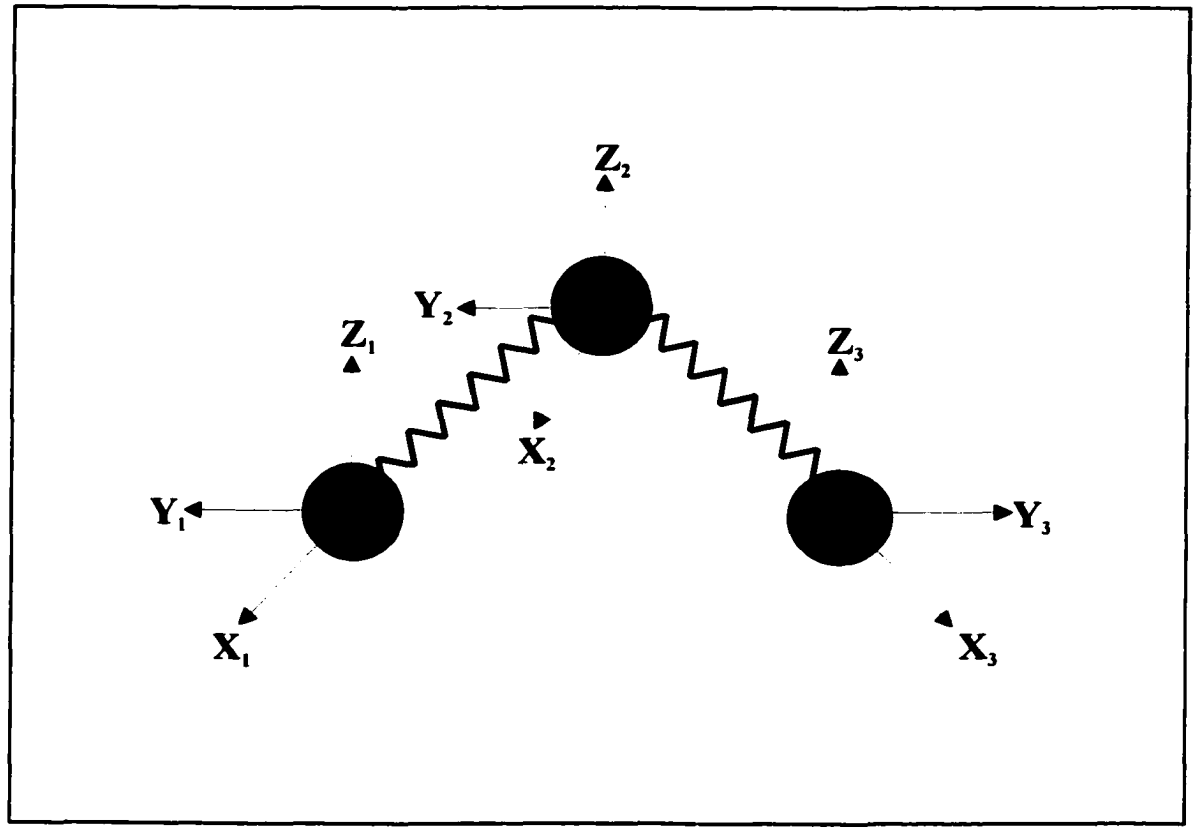

Figure 1. Normal Mode Analysis assumes that atoms are point masses that are held by a spring that obeys Hook's law **F=-kx**.

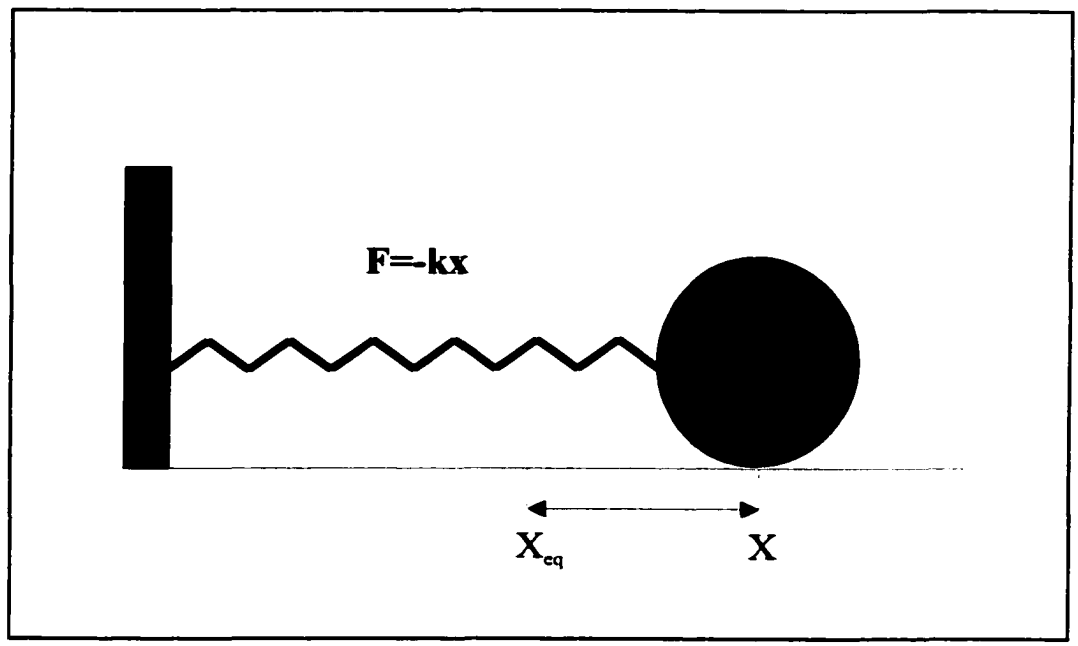

Figure 2. Motion of a body under influence of a force exerted by a spring.

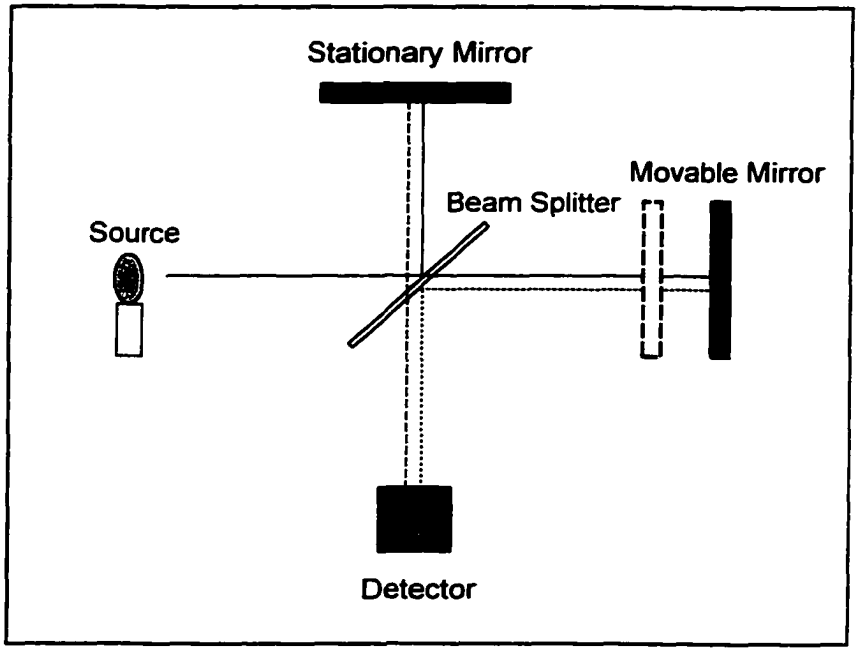

Figure 3. A Diagram of Michelson's Interferometer.

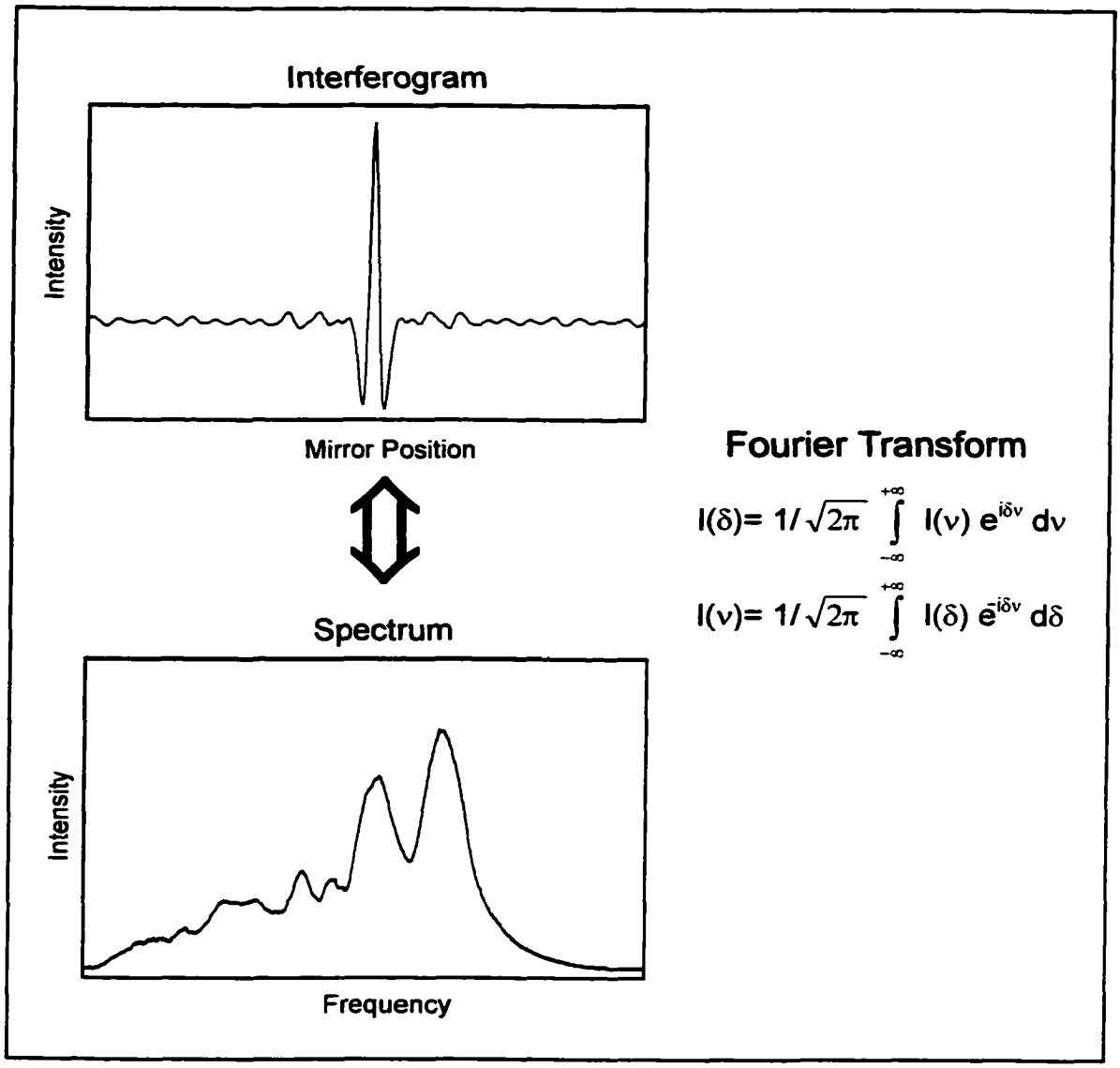

Figure 4. An interferogram is converted to a spectrum by Fourier Transform.

Chapter 2: The Effects of Hydration on Proteins Spectra

Abstract: The infrared absorption spectra of three sample proteins as dry, lyophilized powders in KBr pellets, as hydrated proteins in KBr pellets, as hydrated or dehydrated films, and in solution phase are reported. An enormous increases in the absorption intensities of the amide I and amide II vibrations was noticed between the dry and the hydrated phases. This intensity enhancement was observed by hydrating proteins with both H_2O and D_2O. Observed intensity changes between dry and hydrated protein samples were interpreted in terms of variations in the dielectric constant of the immediate surroundings of the peptide linkages.

Proteins have the greatest contribution to the infrared spectrum of a cells or tissues. Therefore, the effect of hydration/dehydration on the infrared spectra of proteins, will be discussed first. The spectral changes observed between dry, hydrated and completely dissolved proteins, as well as the method that was developed to study hydration will be described in this chapter.

2.1 The Hydration Procedure

The method that was developed to study hydration utilizes KBr pellets as sample medium . KBr comes in a form of white powder. It is an infrared transparent material with an infrared transparent wavenumber range from 400-5000 cm^{-1}. This compound is primarily used for acquisition of infrared spectra of solids. A KBr pellet is prepared by pressing a mixture that consist of finely ground analyte (protein) and KBr . The quality of a produced pellet is judged by it is transparency. The semi-transparent or poorly transparent pellet usually results from a poor grinding, or from the application of inadequate pressure. To produce a proper KBr disc it is necessary to know the exact KBr /sample mass ration, and the amount of pressure to applied. All this parameters are determined

by trial and error and usually depend on the press that is available to a spectroscopist.

Hydration of the solid proteins was studied in a qualitative manner by first producing a KBr pellet of the dried protein and subsequently hydrating the pellet at room temperature in a water-saturated atmosphere for 10 and 20 minutes. The experimental setup is shown on Figure 1. Different pellets prepared from the same KBr/sample mixture were used for 10 minutes and 20 minutes hydration experiments. The spectra of dry and hydrated protein pellets were baseline corrected, smoothed, normalized and then compared.

Prolong exposure of the pellet to water vapor degrades the pellet and quality of spectra significantly. Upon hydration, KBr-protein pellet turns from transparent to white. As a result, a pellet scatters more light producing a sloping baseline. In addition spectra become noisier. Therefore, it was necessary to subject all pellet spectra to a baseline correction and smoothing algorithms. To normalized spectra, the bands in a protein spectrum that is thought to be invariant to the hydration effect were chosen. Because of the hydrophobic nature of CH_3 and CH_2 groups of amino acid side chains, vibrations of these groups were used for normalization.

The experiments described were purely qualitative in nature, since it was not possible to establish the amount of water absorbed by the pellets. However, the hydration was found to be reversible and reproducible.

2.2 Materials and Methods

The proteins used in this study were human serum albumin, a predominantly α-helical protein, α-chymotrypsin from bovine pancrease, a protein that has a large β-sheet content and type III collagen, a protein with a triple helical structure. All proteins were purchased form Sigma Chemicals, Inc., in form of lyophilized powders and used without further purification. In this work, the lyophilized sample was assumed to be the driest form of a protein. The samples were stored in accordance with the guidelines specified by the manufacturer and in containers with desiccant. For all solutions distilled water was used as a solvent. All work was conducted at room a temperature
(25 °C).

The spectra of dry and hydrated KBr pellets of proteins were collected on either a Vector 22 or IFS 28/B (Bruker Optics, Billerica, MA), a BOMEM MB 100 (BOMEM, Quebec, Canada) or a MIDAC Series M (Midac, Inc, Costa Mesa, CA) FT-IR spectrometer using DTGS detectors . The spectral measurements were repeated on several of the spectrometers listed above, and excellent reproducibility of the hydration results was observed between the different instruments. Spectra were collected at 2 cm^{-1} resolution and for each spectrum 100 interferograms were co-added. Fourier transformation was carried out with Mertz phase correction function and 3-point Blackman –Harris apodization algorithm. All spectra were subsequently smoothed with 15-point Savitsky-Golay [1] . The spectrum of pure KBr pellet was used as a background. The procedure of hydration experiments is outline in section 1.1. The pellets in the hydration studies used a

KBr : albumin ratio of 150 : 1 , KBr: chymotrypsin ratio of 300:1 and KBr : Collagen ration of 150:1 by mass, and were produced by a hand-held press. The weight of a pellet was 30 mg , diameter 7.48 mm and 0.38 mm thickness.

The absorption spectra of the proteins in aqueous solution (at 20 and 40 mg/mL, for albumin and chymotrypsin, respectively) were acquired on Bruker IFS 28/B (Bruker Optics, Billerica, MA) FT-IR spectrometer using a DTGS detector. The liquid sampling cell was constructed with a 5 μm Teflon spacer and BaF_2 windows. Data were collected at 2 cm^{-1} resolution, and 256 interferograms were averaged for each spectrum. Interferograms were Fourier transformed using the same phase correction and apodization fuctions as for pellet spectra. The spectrum of pure water was used as the reference spectrum. Spectra were corrected for residual liquid water contributions following a procedure due to Mitchell *et al.*, [2]. The spectrum of water was iteratively subtracted from protein spectrum until the appearance of a straight baseline in a 1750-1900 cm^{-1} region.

The spectra of human serum albumin and α-chymotrypsin films were recorded on Bruker IFS 28/B (Bruker Optics, Billerica, MA) FT-IR spectrometer using DTGS detector at 2 cm^{-1} resolution and by co-adding 100 scans. Interferograms were Fourier transform using the same phase correction and apodization functions as for pellet spectra. The spectrum of BaF_2 window was used as a background. The sample films were prepared by casting a drop of 20 mg/mL aqueous human serum albumin or α-chymotrypsin solution onto BaF_2 window and placing the sample into a vacuum for one and a half-hours. After spectral

acquisition, this film was treated with about 150 μL of pure ethanol and dried in a vacuum for a same amount of time.

2.3 Results

Figure 2A, trace a-d, shows the FT-IR absorption spectra of dry, polycrystalline albumin, hydrated albumin and an aqueous solution of albumin, respectively. Figure 2B shows an expanded view of the amide I / amide II region of spectra a and d. The spectral changes between traces a and c are reversible and completely reproducible. The rounded band shapes observed for the dry albumin in the amide I and amide II bands at 1655 and 1540 cm^{-1}, respectively, are not due to non-linear detector response due to excessively high absorption values. This was demonstrated by collecting these data over a broad range of KBr : protein ratios. This concentration study did show unambiguously that these band shapes are not an artifact, but represent the true and inherent band shapes of the dried, polycrystalline protein.

Upon hydration of the protein-containing KBr pellet, a reversible increase and sharpening of the amide I and amide II peaks is observed, with the intensity increase approximately proportional to the level of hydration. An analogous sharpening of both amide peaks is also seen for chymotrypsin and collagen, a protein with a very unique secondary structural motif called triple helix (Figures 3a-d and 4a,b). Thus, the observed hydration effect is independent of the predominant secondary structure of a protein.

In order to demonstrate that the peak sharpening is not merely due to the presence of the water deformation mode at *ca.* 1635 cm^{-1}, two experiments were carried out. One of these used D_2O, instead of H_2O for hydration of the protein. The result of this study is shown in Figure 5. The spectra reveals that hydration of an albumin pellet with D_2O produces an intensity enhancement in the amide I band that is very similar to that seen for hydration with H_2O. Thus, the variation in band shapes of the amide I and II bands is due to a hydration of the protein, and not merely the superposition of the water deformation band on the amide I and II envelopes. This was further demonstrated by modeling band shapes in the amide I / amide II region. To this end, an appropriately scaled liquid water spectrum was added to a spectrum of dry protein (Figure 6). The simple superposition of water and protein spectra did not reproduce the changes observed in the amide I and II spectral regions and most importantly variation in amide III band shape observed for proteins. Thus, we conclude that the different band shapes observed upon hydration are due to water molecules solvating the amide linkages. Yet, the amount of water absorbed by the pellet was so small that it could not be detected gravimetrically.

In order to demonstrate that the observed spectral changes do not result from a pressure-induced denaturation of the protein (after all, the pellets are produced by compressing KBr-sample mixture under high pressure), we also investigated protein hydration / dehydration effects using films. Figure 7and 8 shows the unnormalized spectra of protein films before and after dehydration. The ob-

served spectral changes reproduce the hydration effects observed for the pellets. Additional hydration experiments with protein films are described in chapter 4.

For the studies involving pellets, the same pellet was used for studying the dry and the hydrated protein. Thus, we may assume that the total protein content of the sample did not change. Certain protein peaks, in particular those associated with the non-polar moieties of the protein (*i.e.,* the side group vibration at 1455 cm^{-1}), stayed constant during the hydration experiment. The vibrations associated with the polar amide linkage, on the other hand, showed intensity enhancement upon hydration. For albumin and chymotrypsin amide III mode at 1245 –1305 cm^{-1} showed the smallest intensity variations upon hydration, however for collagen, the change in the band shape of amide III is much more pronounced indicating a structural transformation upon hydration. For all proteins thought, the amide I mode nearly doubles in intensity and becomes much narrower. Similarly, the amide II increases in intensity and shifts to slightly higher frequencies upon increasing hydration (*cf.* Table I).

Figure 2 and 3 also shows that the hydration of the proteins in the KBr pellet produces spectra that lie between the dry pellet and the protein aqueous solution. The intensity ratio of the amide I / amide II bands is about 2 for albumin and chymotrypsin in aqueous solution, measured in transmission mode. This intensity ratio is similar to the one observed generally for proteins and also for cells and tissues.

2.4 Infrared Spectrum of Protein: Bands Assignment

The infrared spectrum of proteins is rather complicated: however, there are number of vibrational modes the origin of which are well know and well understood. These are the amide I , amide II and amide III vibrations of the peptide moiety of a proteins. The diagram below shows the structure of a peptide linkage.

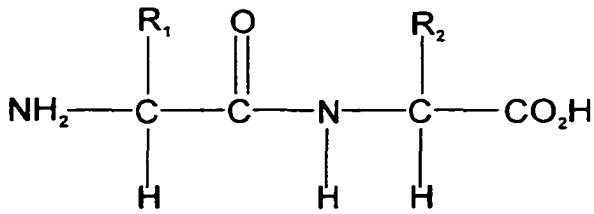

Peptide Linkage

The amide I vibration in a single amide linkage is predominantly due to C=O stretching coordinate with small N-H stretching and C-N stretching contributions. The vibration of the carbonyl group in a protein is observed somewhere between 1630 to 1700 cm^{-1}. This mode is sensitive to a secondary structure of a protein and is often used to estimate relative amounts of different secondary structure that may be present in a protein. The amide II vibration is produced largely by N-H in plane bend that oscillates out-of-phase with C-N stretching vibration and is observed around 1540 cm^{-1}. The N-H vibration accounts for 49 percent of potential energy of amide II vibration , whereas C-N stretching motion contributes 33 percent [3]. The assignments of the peptide linkage vibrations come from the analysis of molecules with amide groups [4-6]. The amide III vibration in protein is

due to coupling of N-H and methine deformation (methine hydrogen in peptide linkage is circled). This was determine by Odoodi et al., through a studies of deuterium substituted L-AlA-L-Ala [7]. This assignment was recently confirmed by deep UV resonance Raman studies of a number of model peptides [8].The amide III is also known to be sensitive to the conformation of a protein, however this particular vibration is rarely used for a structure determination.

It is a prevalent assumption among most vibrational spectroscopists today that unique shape of amide I envelop in a protein is purely due to various type of hydrogen bonding patterns in a protein [9]. Thus, one argues that α-helix is observed at around 1650 cm^{-1} because of one type of hydrogen bonding, β-sheet around 1680 cm^{-1} because of the other, and random coil at around 1690 cm^{-1} because of a third type. Indeed, hydrogen bonding plays an important role in stabilizing a protein structure. However, from infrared spectroscopy point of view "hydrogen bonding" may not the best model for rationalizing the protein spectra. It may explain why C=O band in predominantly α-helical protein is observed at 1650 cm^{-1} : however, the same model fails to explain why β-sheet structure produces vibrations at *ca.* 1635 cm^{-1} and at the same time at *ca.*1680 cm^{-1}. The " exciton coupling" that will be described next may be a better approach for explaining amide I band of infrared spectra of protein.

2.5 "Exciton Coupling" Model

This model explains unique shape of amide I band in a protein in terms of interaction or coupling of transition dipole moments of individual C=O vibrations

of a peptide linkages in a protein (Figure 9). The singly excited C=O vibrational states couple, and the whole excitation becomes delocalized. It this point we can not talk anymore about individual C=O vibration but should rather focus on one delocalized excitation that is spread over a particulate region of a protein molecule . The coupling produces the energy splitting –exciton splitting. It can be shown that for a dimer ,a molecule with two interacting vibrations, the frequencies of two new transitions produced by the exciton coupling are

$$\nu_+ = \nu_0 + V_{12} \qquad \textbf{eq.1}$$

$$\nu_- = \nu_0 - V_{12}$$

In this equation ν_0 is the frequency of the unperturbed transition. V_{12} is the energy of interaction between individual transition dipoles in a dimer. It is evident from the equations that coupling produces one new state with higher frequency that the unperturbed transition and one with lower frequency. The potential energy of interaction V_{12} of two excited states on the other hand depends on a) the strength of transition dipole moment of vibration b) relative orientation of two transition dipoles to one another and c) distance between two transition dipoles.

$$V_{12} = \frac{\mu_1 * \mu_2}{R^3} - 3 * \frac{(\mu_1 * R)(\mu_2 \cdot R)}{R^5} \qquad \textbf{eq.2}$$

μ_1 and μ_2 are transition dipoles moment of individual vibrations respectively, and R is the distance between two interacting excited states [10]. For general case, where more than two transitions are involved in coupling , equation 2 becomes

$$V_{IJ} = \frac{\mu_I * \mu_J}{R^3} - 3 * \frac{(\mu_I * R_{IJ})(\mu_J \cdot Rij)}{R^5} \qquad \textbf{eq.3}$$

Thus, geometry of interacting transition dipoles and the distances between them become a very important factor in the absorption process of protein. The different wavelengths observed for different types of secondary structure in protein are due to relative orientation of carbonyl groups in one type of secondary motif vs. the other. The commonly found statement that the amide I mode of α-helical proteins occurs at 1655 cm^{-1}, and that of β-sheets at 1635 and 1680 cm^{-1}, should really be viewed as different "exciton", or coupled-state contributions [11]. Recent FT-IR and VCD studies on ^{13}C substituted peptides [12,13] have demonstrated that the interactions giving rise to the conformational sensitivity can be described in terms of different coupling interactions of the amide I transition moments becoming dominant at different interaction geometries. Due to the relatively small dipole change of the amide I transition moment the interaction coupling the individual amide I transition into a delocalized manifold of bands is restricted to small distances, perhaps five to ten amide linkages.

2.6 Intensity variations upon hydration

The band intensities (heights), band width and integrated intensity of the amide I and amide II peaks for dry pellets, hydrated pellets and aqueous solutions of both proteins are summarized in Table I. In this Table, the reported intensities were determined as follows. Peak heights of the amide I and II bands were obtained for spectra normalized at 1452 (albumin) or 1387 cm^{-1} (chymotrypsin). Integrated peak intensities were estimated by fitting a single Gaus-

sian/Lorenzian (50:50) peak to each of these bands, and evaluating the integrated intensities from the half width and heights of the component bands (Figure 10). Two distinct trends can been seen as the state of hydration of a protein increases. First, the integrated intensities and peak heights of both amide I and II bands increase with hydration, and second, the band widths become progressively narrower going from dry state to solution. These two trends will be discussed next.

The variation in integrated intensity, and the shape of the amide bands is most likely due to both a change of the dielectric environment of the peptide linkage, and slight structural modification that protein may undergo when water molecules are added. The integrated intensity (the area under the absoption band) is given by [14] :

$$A_{integrated} = \{\pi Na / 3c^2\} \ (\partial\mu / \partial \mathbf{Q})^2 \qquad \textbf{eq.4}$$

where Na is Avogadro's Number, c is the velocity of light and ($\partial\mu / \partial \mathbf{Q}$) is the change in the transition dipole moment with the normal coordinate. According to equation 1, the integrated intensity is proportional to the square of the dipole moment change, and inversely proportional to the square of the speed of light, which, in turn, is a function of both dielectric constant ε and the magnetic susceptibility, μ of the medium [15]:

$$c = 1/\sqrt{\varepsilon\mu} \qquad \textbf{eq.5}$$

The dielectric constant of water is expected to be higher than the dielectric of the solid protein, which may explain the increase in the intensity of the amide I band.

The enhancement in peak intensity between the dry pellet and the aqueous solution, appears to represent an increase in the local dielectric environment that the amide linkage experiences upon hydration.

Fujiyama and Crawford [16] presented theoretical and experimental evidence that the dielectric effect can change the local strengths of the light that interacts with a molecule and alter band shapes and intensities . This was accomplished by studying liquid hexaflourobenzene (C_6F_6) spectrum and then comparing results with the gas phase spectrum of C_6H_6. Hexaflourobenzene was chosen because molecules of this substance have minimal intermolecular interactions in the liquid phase. Therefore they argue that integrated intensities of bands determined from liquid spectrum and gas spectrum of C_6H_6 should be similar.

To determine how a dialectic effect influences the properties of infrared bands of liquids they proceeded in a following way. First, they obtained an ATR spectrum of C_6H_6 . Attenuated Total Reflection (ATR) is an infrared sampling technique primarily used to measure infrared spectra of liquids. Using ATR it is possible to obtain absorption spectrum a sample or ***k*** *spectrum* and refractive index ***n*** of a sample. In other words, ATR allows determining simultaneously both parameters of the complex refractive index $\hat{\eta}$

$$\hat{\eta} = \eta + \imath\kappa \qquad \textbf{eq.6}$$

where η is a refractive index and κ is extinction coefficient . Both η and κ are function of frequency, and change values considerably when measuring at the absorption band.

Figure 11 shows both ***k*** and ***n*** spectra for 1527 cm^{-1} fundamental carbon-carbon benzene ring vibration in liquid C_6H_6.

To incorporate dielectric field effects in liquid spectra Fajiyama and Crawford had adapted the Lorenz-Lorentz approximation for their calculations. Lorenz-Lorentz approximation related local field E_{local} that molecule experience to the macroscopic electric field E by

$$E_{local} = E - (4\pi/3)\, P \qquad \textbf{eq.7}$$

where P is the polarization of dielectric. This equation can also be written as

$$1/C=(1/\chi) - (4\pi/3) \qquad \textbf{eq.8}$$

C is the local susceptibility, which relates the response of a molecule to the local field and χ is the macroscopic susceptibility. Since χ relates directly to $\hat{\eta}$, the local susceptibly is

$$C = C' + iC'' \qquad \textbf{eq.9}$$

Fujiyama and Crawford then derived the expression for extinction coefficient that takes a dielectric effect into account

$$\kappa_0=2\pi C'' \qquad \textbf{eq.10}$$

Once they had established the relationship between ***k*** and k_0, the ***k*** spectrum was corrected for dielectric effect to obtain k_0 spectrum . On Figure 11 ***k*** spectrum and k_0 spectrum (the spectrum corrected for dielectric effect) are compared. The changes in a band shape are obvious. The integrated intensities for both spectra were also computed. The *uncorrected integrated intensity* was evaluated using the following equation

$$A_{integrated}\ (\text{uncorrected}) = (4\pi/c_m) \int \kappa(\bar{\nu})\, d\bar{\nu} \qquad \textbf{eq.11}$$

c_m is molar concentration and *correct for dielectric effect integrated intensity* from,

$$A_{integrated}\ (corrected) = (8\pi/c_m) \int k_0\ (\bar{\nu})d\bar{\nu} \qquad \textbf{eq.12}$$

It was found that uncorrected integrated intensity derived from ***k*** spectrum is bigger then integrated intensity derived form corrected for dielectric effect k_0 spectrum by 20%. The change in local dielectric causes increases in integrated intensity by 20 % for hexafluorobenzene. Moreover, Fujiyama and Crawford compared integrated intensity computed form corrected for dialectic effect liquid spectrum C_6H_6 with integrated intensity of the same band but computed from gas phase spectrum of the C_6H_6, and found them to be very similar to each other.

The theoretical and experimental work on C_6H_6 demonstrates that a dielectric effect can cause changes in a band shape and integrated intensity. One possible way in which water can enhance the intensity of amide I and amide II vibrations is depicted on Figure 12. Electric field from the source interacts with a water molecule and induces a dipole moment. Water molecule that is in proximity of protein amide linkage will most likely to adapt some sort of fix geometry relative to amide linkage as oppose to being randomly oriented. Water molecules that are present in a structure of a protein and that have a very similar spatial orientation can produce a small electric field. If the electric field vector produced by water molecules has the same orientation as the electric field from the source, then two electric fields will add up.

$$E_{total} = E_{source} + E_{water}$$

Therefore, the total electric field that protein sees when water molecules are present in a structure will be slightly greater in magnitude, compared to a situation when water molecules are not part of the structure. Addition of water molecules increases the electric field that protein perceives which consequently leads to the enhancement of amide I and amide II vibrations.

2.7 Narrowing of the Amide I Bandwidth

The second trend, the narrowing of the width of the amide I band in hydrated samples as compared to the dry protein, is an unexpected result. In general, broad infrared bands are associated with heterogeneity of chemical interactions, and samples having disordered structures. Thus, one should expect the solid phase spectra to exhibit narrower features.

The opposite behavior observed in this particular case - hydration and solvation resulting in a decrease in the width of the amide I band – suggests that the protein undergoes some structural rearrangement when the water content increases. However, it is unlikely that hydration causes a major changes in protein's secondary structure, since the frequency of the amide I band does not shift between the dry and hydrated states. Thus, it is possible that in the dry, polycrystalline protein a broader distribution of conformational angles ϕ and ψ exists. This will result in a broad distribution of conformers of similar energy that may be allowed in the inhomogeneous environment of the polycrystalline solid. This broad distribution of conformational angles between the amide linkages will result in a broadened amide I band.

In the hydrated state, on the other hand, the protein assumes a global energy minimum that permits fewer structures with more narrowly defined conformational angles. The interactions of fewer conformational states, enhanced in intensity by the hydration of the amide linkages, will result in a narrower amide I manifold.

2.8 Estimated Water Uptake of Protein Pellet

The close resemblance between the spectrum of hydrated pellet and the aqueous solution suggests that a relatively small number of water molecules is required to produce a hydration environment of the amide linkage that mimics the totally solvated state. An attempted was made to quantify both the amount of water absorbed by a KBr/protein pellet and by a pure KBr pellet (without protein). The amount of water absorbed by pure KBr pellet is so small that the bulk water spectrum could not be detected spectroscopically. Thus, we conclude that the hydration effect of pure KBr is extremely small. In the case of KBr / protein pellets, the broad water overtone centered at *ca.* 2150 cm^{-1} was observed weakly, but the water content could not be detected gravimetrically. The precision of the balance that was used to weight pellets was 0.1 mg. However, it had failed to register any change in weight between dry and the hydrated KBr disc. Thus, it was assume that the increase in mass (of a 30 mg pellet) was less than 0.1 mg. Based on this assumption the rough estimate of water intake of a pellet was made. In this calculation 0.1 mg was taken as an upper limit of a water uptake of a pellet (Figure 13). From this calculation and experimental data that shows a

great similarity between the spectrum of hydrated pellet and the spectrum of aqueous solution it is evident that a finite number of a water molecules rather than a bulk hydrated the protein.

Unfortunately, there is little literature precedence for infrared intensity variations under the influence of the local dielectric. However, *ab initio* calculations of the vibrational spectra of aqueous solutions at the B3LYP/ 6-31G* level of N-acetyl-L-alanine N'-methyl amide (AAMA)

$$CH_3\text{-}CONH\text{-}CHCH_3\text{-}CONH\text{-}CH_3,$$

a peptide model compound with two peptide linkages attached to an alanine residue, required the presence of four explicit water molecules to stabilize conformers of AAMA that are not stable in the isolated state [17]. In addition, calculations show that water molecules effect the geometry of model compound, and that interactions between solvent and solute molecules in the vicinity of the amide linkages strongly influence the vibrational spectrum of AAMA. Thus, the conclusion was made that water molecules, diffusing into the KBr pellet containing protein microcrystals, predominantly hydrate the peptide linkage, which is among the most polar moieties in a protein. If, indeed, just a few water molecules in the vicinity of the peptide linkages are required to influence the amide I and II absorption intensities, then the amount of water in sample will be too small to be detected gravimetrically.

For pellets, it is known that shapes of IR bands depend on the degree of grinding. Large particles produced by inadequate grinding of the pellet material will strongly scatter the light, leading to distortion of the true band shape. How-

ever, the results reported here emphasize to a lesser degree the shape of bands, but rather, the intensity variations of the vibrations of the polar bands in the proteins, as compared to those of non-polar groups. In addition, these changes are also observed between solids and solutions, and hydrated and dry films.

Conclusion

Two conclusions can be derived from the result presented in this chapter. First, the intensity and shape of the amide I band and to a lesser extend amide II and amide III are effected by presence of water in a protein. And second, a finite number of water molecules as oppose to bulk is needed to simulate the fully hydrated state of a protein.

References

1. Savitsky,A.; Golay,M,J,E. Smoothing and Differentiation of Data by Simplified Least Squares Procedures. *Anal.Chem* . **1964**, 36 (8), 1627-1639.

2. Mitchell, R. ; Harris, P,I.; Fallowfield,C. ; Keeling,D,J.; Chapman C. Fourier transform infrared spectroscopic studies on gastric H^+/K^+-ATPase. *Biochem. Biophys. Acta.* **1988**, 941, 31-38.

3. Miyazawa,T.; Shimanouchi ,T.; and Mizushima, S. Normal vibrations of N-methylacetamide. *J.Chem.Phys.* **1958**, 29,611-616.

4. Miyazawa,T. Characteristic Amide bands and conformations of polypeptides. In *Polyamino acids,Polypeptides and Proteins*. Stahmann, M, A.,Ed. University of Wisconsin Press: Madison, WI, 1962; pp 201-217.

5. Jakes,J.; Krimm S. Normal coordinate analysis of molecules with the amide group. *Spectrochim.Acta. Part A* .**1971**, 27,35-63.

6. Krimm,S.; Bandekar,J. Vibrational spectroscopy and conformation of peptides,polypeptides and proteins. *Adv.Protein.Chem.* **1986**,38,181-363.

7. Oboodi M.R.; Alva, C.; Diem,M. Solution-Phase Raman Studies of Ananyl Dipeptides and Various Isotopomers: A Reevaluation of Amide III Vibrational Assignment. *J.Phys.Chem.* **1984**,88,501-505.

8. Asher, S,A.; Lanoul, A.; Mix, G.; Boyden,M.; Karnoup,A.; Diem,M.; Schweitzer- Stenner,R. Dihedral Angle Dependence of the Amide III Vibration: A Uniquely Sensitive UV Resonance Raman Secondary Structural Probe. *J.Amer.Chem.Soc.*, submitted (2000).

9. Jackson, M.; Mantsch H,H. The use and misuse of FTIR Spectroscopy in the determination of protein structure. *Crit.Rev.Biochem.Mol.Biol.* 30 (2), **1995**,95-120.

10. Cantor,C,R.; Shimmel P,R. Absorption spectroscopy. *Biophysical Chemistry Part II: Techniques for the study of biological structure and fucntion.* W.H.Freeman and Company: New York,1980; pp 349-408.

11. Diem, M. Biophysical Applications of Vibrational Spectroscopy. *Introduction to Modern Vibrational Spectroscopy.* Jonh Wiley & Sons: New York, 1993; pp 204-225.

12. Silva, R.A.G.D.; Kubelka,J.; Bour, P.; Decatur.; Keiderling,T,A. Site-specific conformational determination in thermal unfolding studies of helical peptides using vibrational circular dichroism with isotopic substitution. *Proc.Natl. Acad.Science.* **2000**,97(15), 8318-8323.

13. Brauner, J.W., C.Dugan and R.Mendelsohn. ^{13}C Isotope Labeling of Hydrophobic Peptides. Origin of the Anomalous Intensity Distribution in the Infrared Amide I Spectral Region of β-Sheet Structures. *J.Amer.Chem.Soc.* **2000**, 122 (4), 677-683.

14. Brown, T.L.; Infrared Intensities and Molecular Structure. *Chem.Rev.* **1958**, 58, 581-609.

15. Halliday,D.; Resnick,R.; Walker,J. Electromagnetic Waves. *Fundamentals of Physics.* 4th Ed; John Wiley & Sons: New York, 1993; Vol 2, pp 988-1010.

16. Fujiyama,T:Crawford,B,Jr. Vibrational Intensities.XXI.Some Band Shapes and Intensities in Liquid Hexaflourobenzene. J.Phys.Chem. **1968**, 72, 2174-2181.

17. Han, W,G.; Jalkanen K,J,; Elstner, M.; Suhai,S. Theoretical Study of Aqueous N-Acetyl-L-alanine N'- Methylamide: Structures and Raman, VCD, and ROA Spectra. *J.Phys.Chem. B.* **1998,** 102, 2587- 2602.

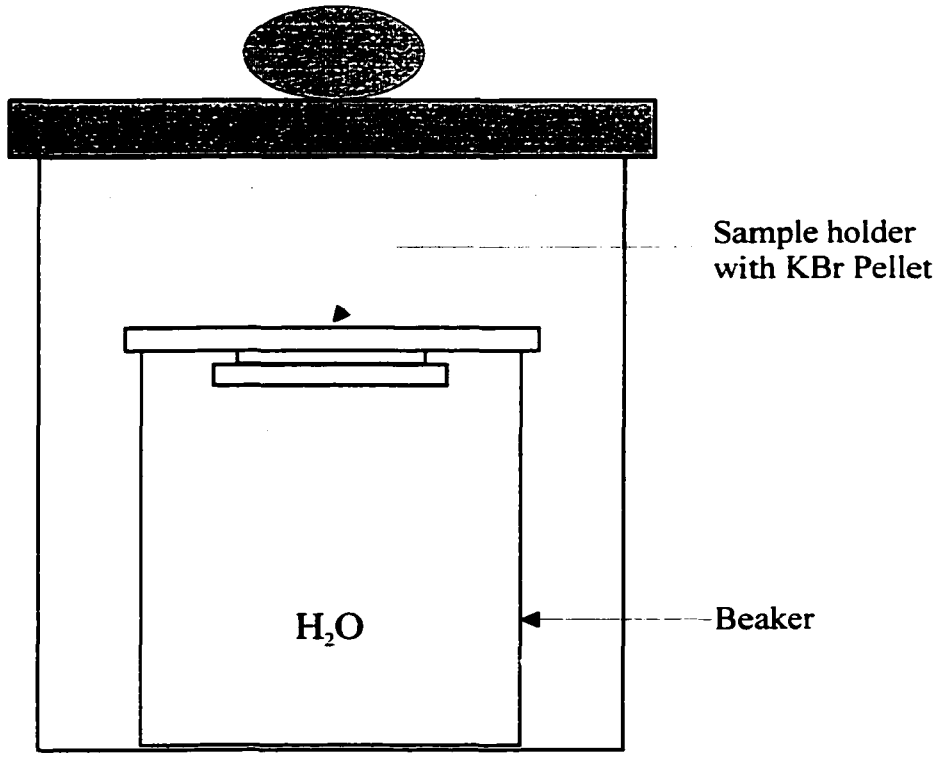

Figure 1. Setup of KBr pellet hydration experiment. The sample holder with KBr disc is placed on a top of the beaker with water that is inclosed in an air-tide vessel .

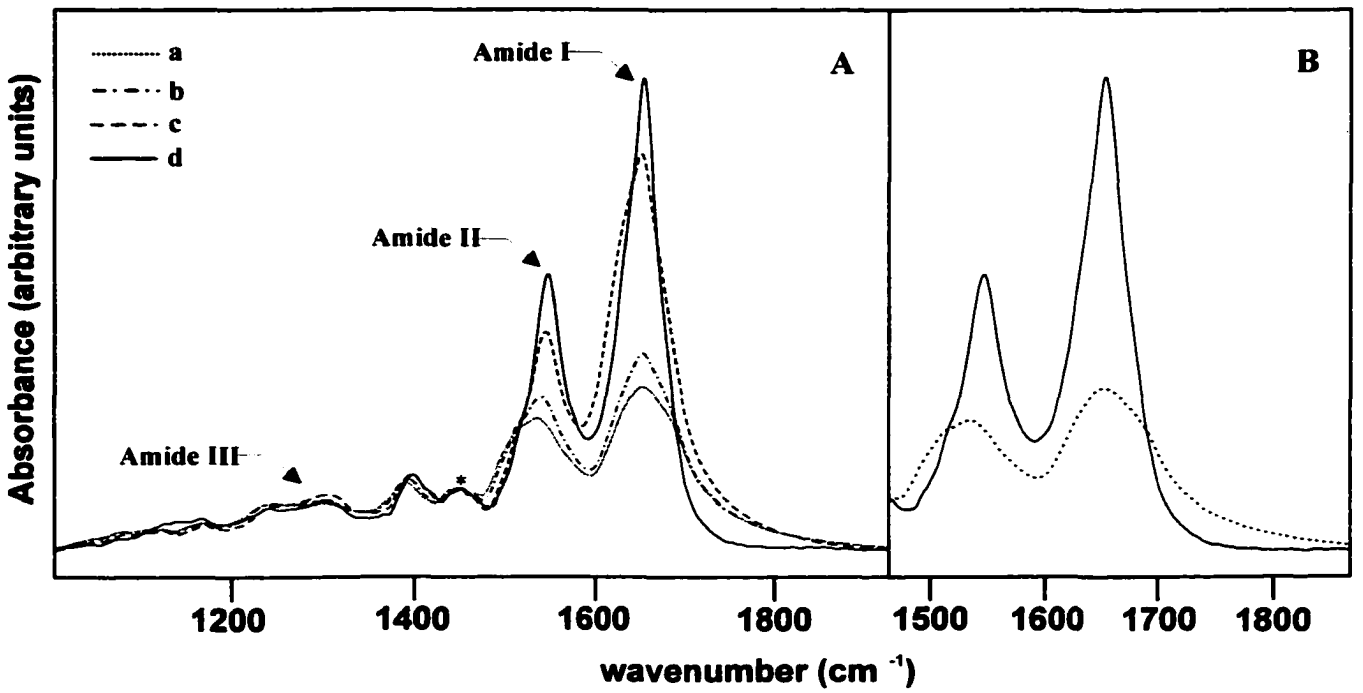

Figure 2. A) FT-IR absorption spectra of albumin. Trace a: dry protein in KBr matrix (1:150, by mass); trace b; protein in KBr matrix (1:150, by mass) after exposure to water vapor for 10 minutes; trace c) protein in KBr matrix (1:150, by mass) after exposure to water vapor for 20 minutes ; trace d) as an aqueous solution (2%w/w), measured in transmission mode at a pathlength of 5 microns. B) expanded amide I/II region of traces a and d. *The spectra were normalized at 1452 cm $^{-1}$.

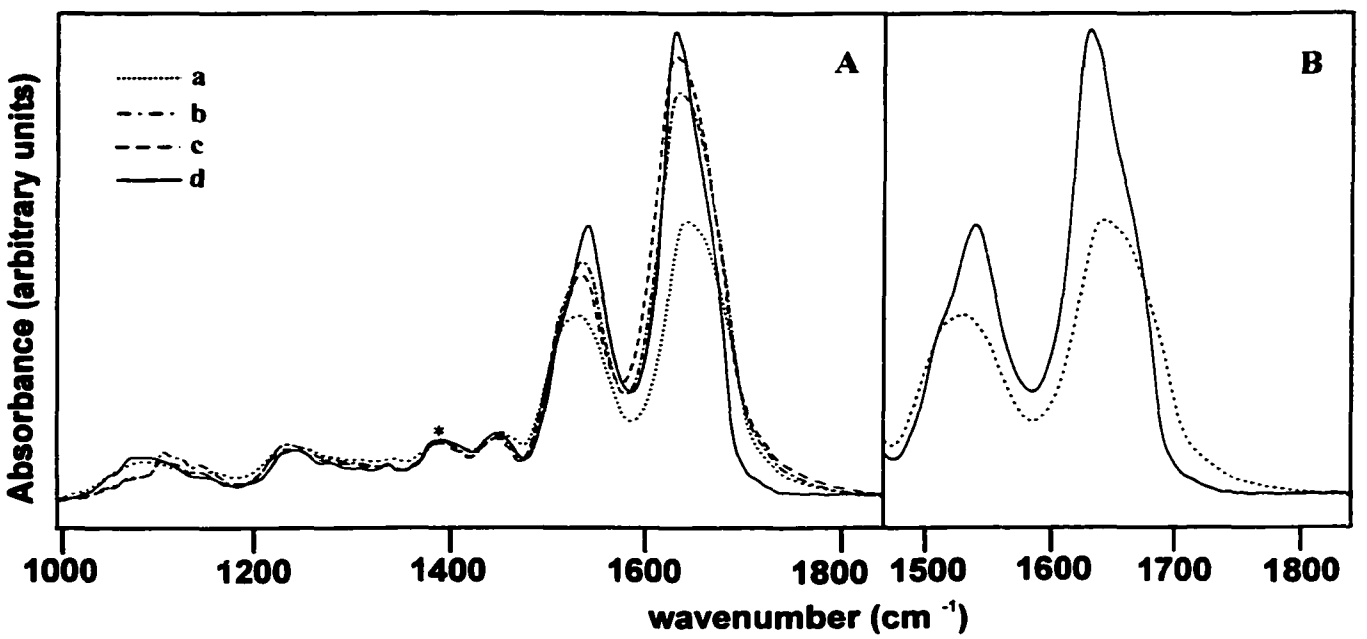

Figure 3. A) FT-IR absorption spectra of chymotrypsin. Trace a: dry protein in KBr matrix (1:300, by mass); trace b) protein in KBr matrix after exposure to water vapor for 10 minutes; trace c) protein in KBr matrix (1:300,by mass) after exposure to water vapor for 20 minutes; trace d) as an aqueous solution (4 % w/w) measured in transmission mode at a pathlength of 5 microns. B) expanded amide I/amide II region of traces a and d. *The spectra were normalized at 1398 cm^{-1} .

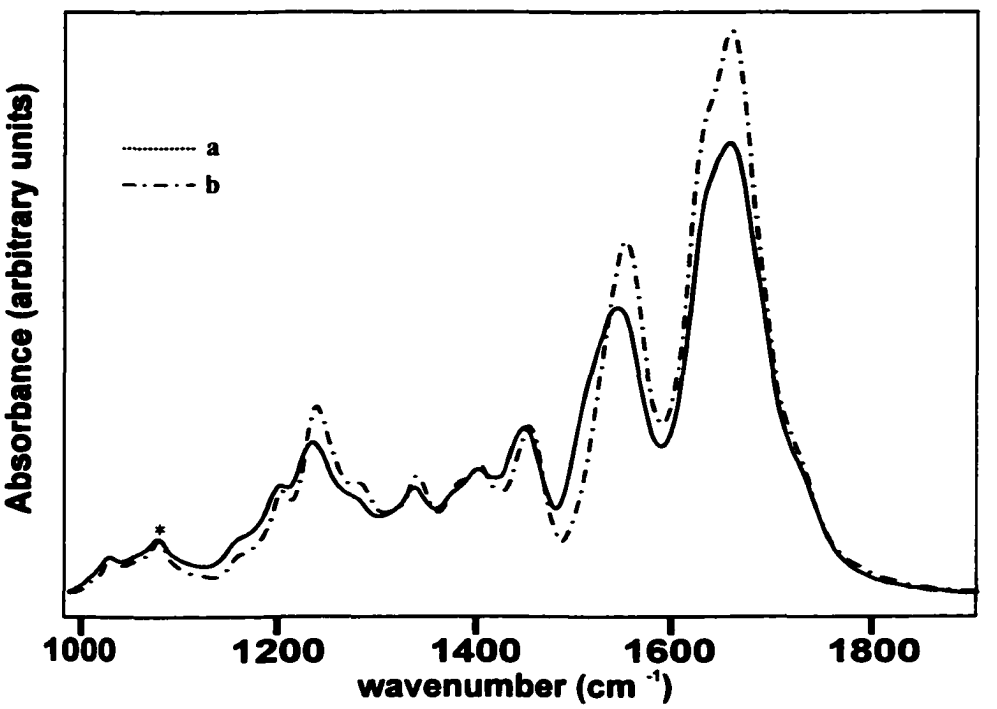

Figure 4. FT-IR absorption spectra of collagen. Trace a) dry protein in KBr matrix (1:150, by mass); trace b) protein in KBr matrix (1:150, by mass) after exposure to water vapor for 20 minutes. *The spectra were normalized at 1082 cm^{-1}.

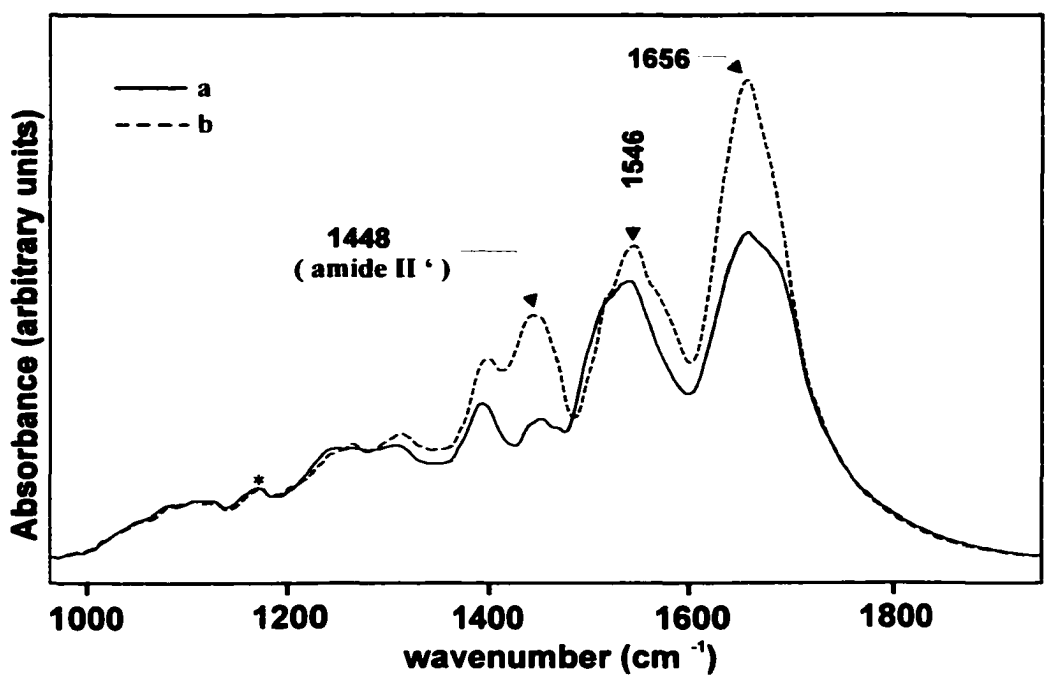

Figure 5. FT-IR absorption spectra of albumin. Trace a) dry protein in KBr matrix (1:150, by mass); trace b) the same KBr protein pellet after an exposure to D_2O vapor for 20 minutes. *The spectra were normalized at 1172 cm^{-1}.

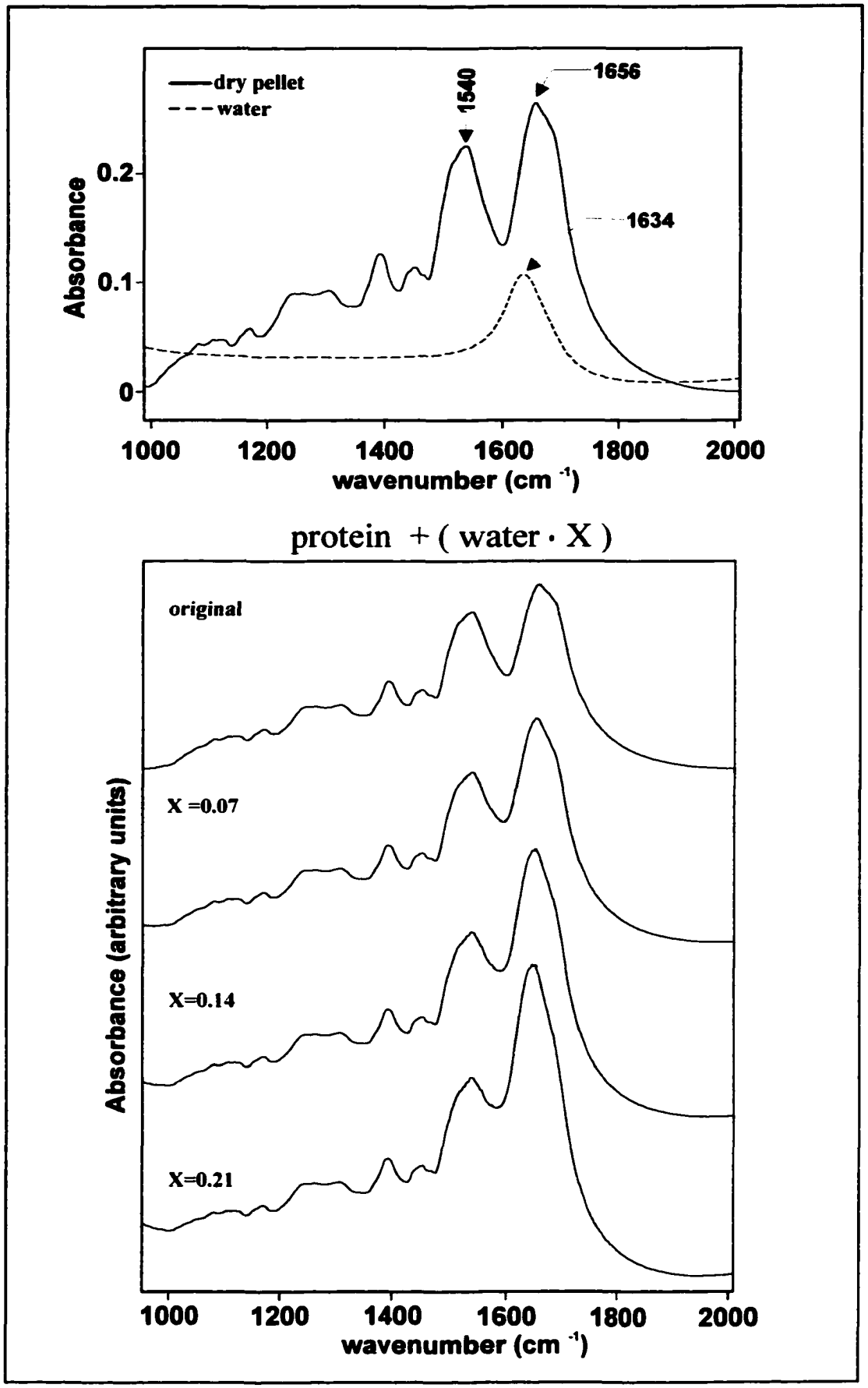

Figure 6. Modeling hydration. Upper figure shows the spectrum of a dry protein and a spectrum of water. Lower figure shows the results of addition of a water spectrum to the spectrum of dry protein.

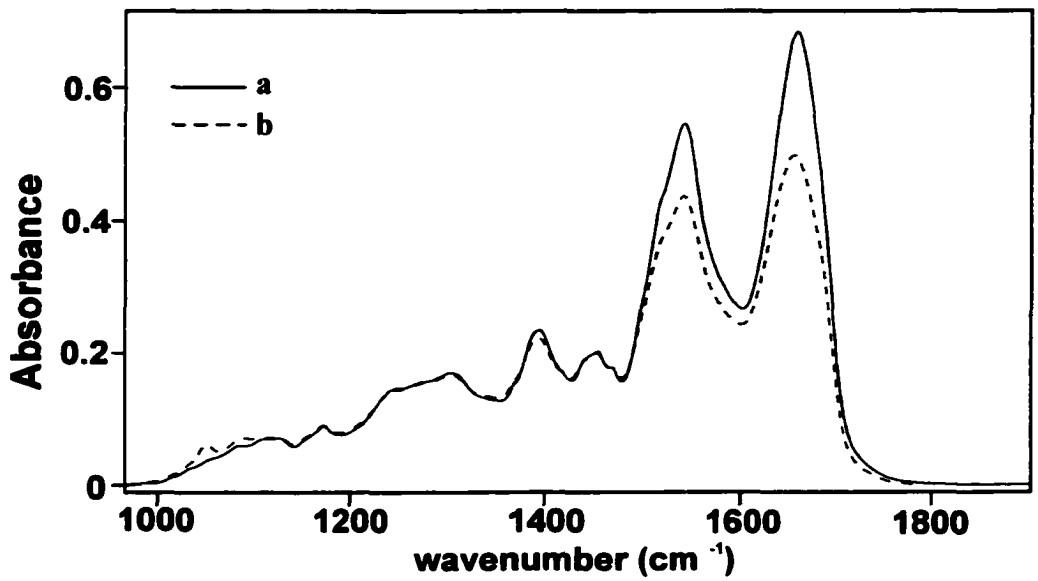

Figure 7. Trace a) FT-IR absorption spectrum of albumin film; trace b) FT-IR absorption spectrum of the same albumin film after the treatment with ethanol. The spectra were not normalized.

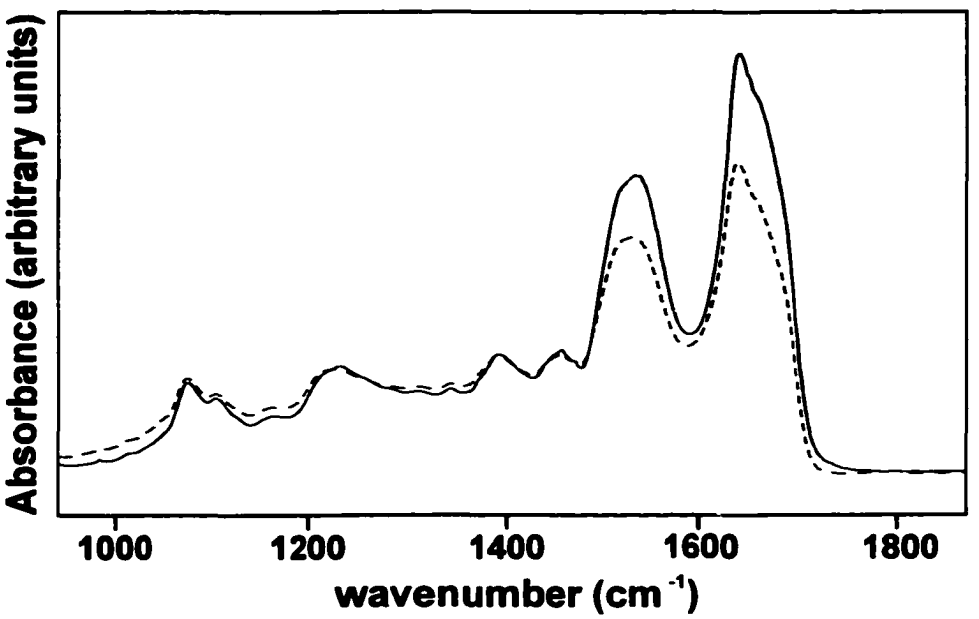

Figure 8. Trace a) FT-IR absorption spectrum of chymotrypsin film trace b) FT-IR absorption spectrum of dehydrated film of albumin (after a treatment with ethanol).

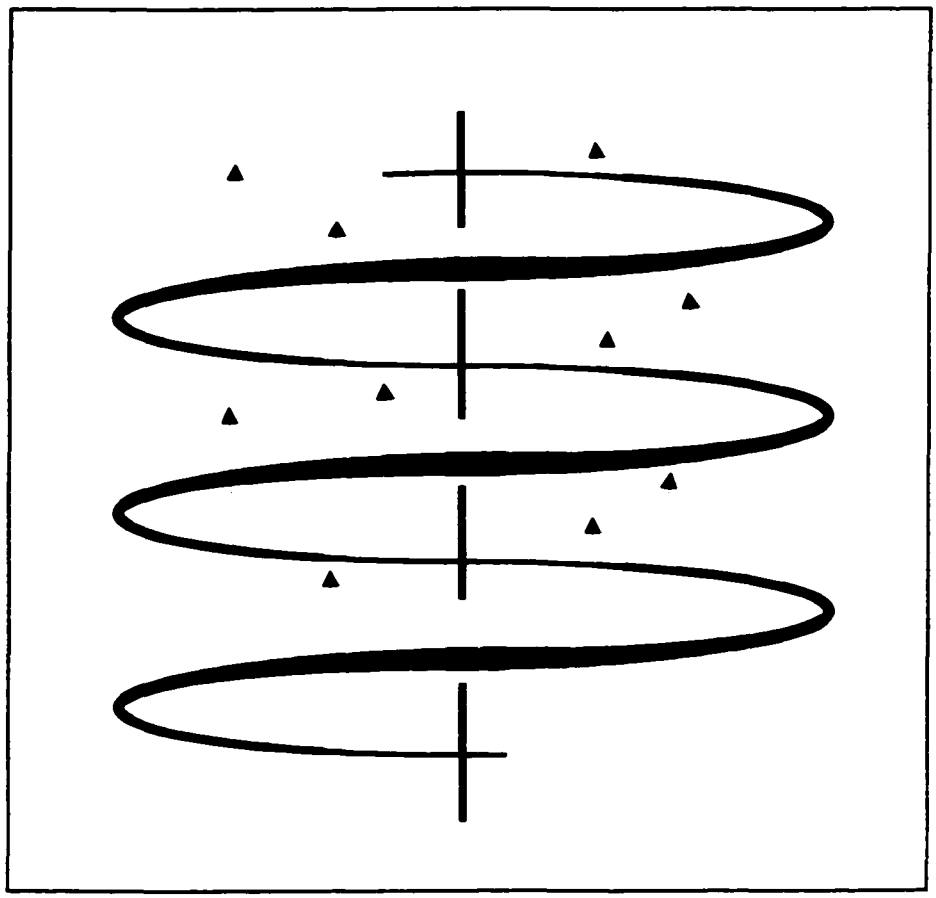

Figure 9. Schematic diagram of protein helix. The arrows represent vibrational transition dipoles.

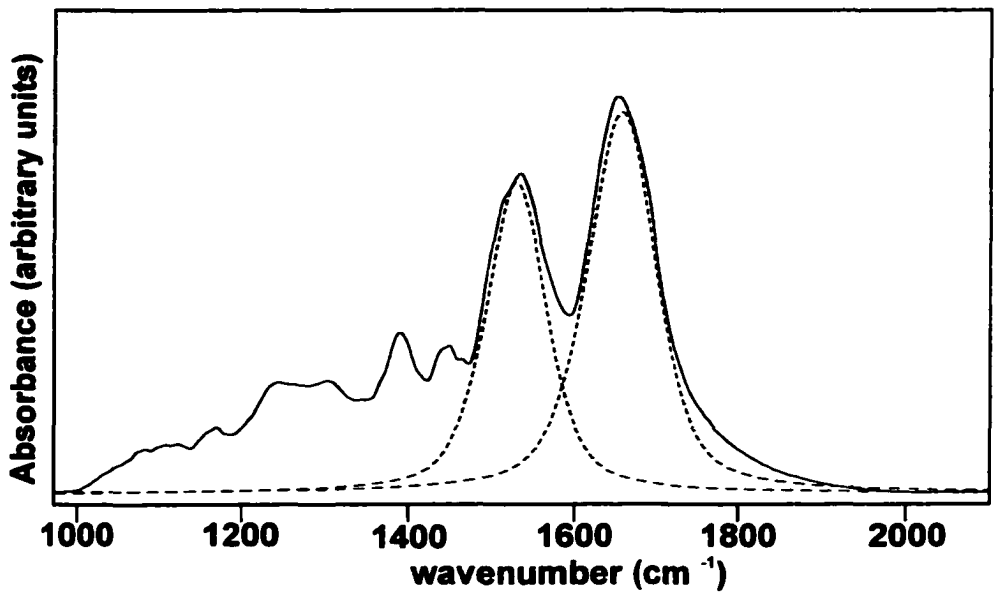

Figure 10. Integrated peak intensities were estimated by fitting a single Gaussian/Lorenzian (50:50) peak shown as dashed traces to amide I and amide II, and evaluating the integrated intensities from the half widths and heights component.

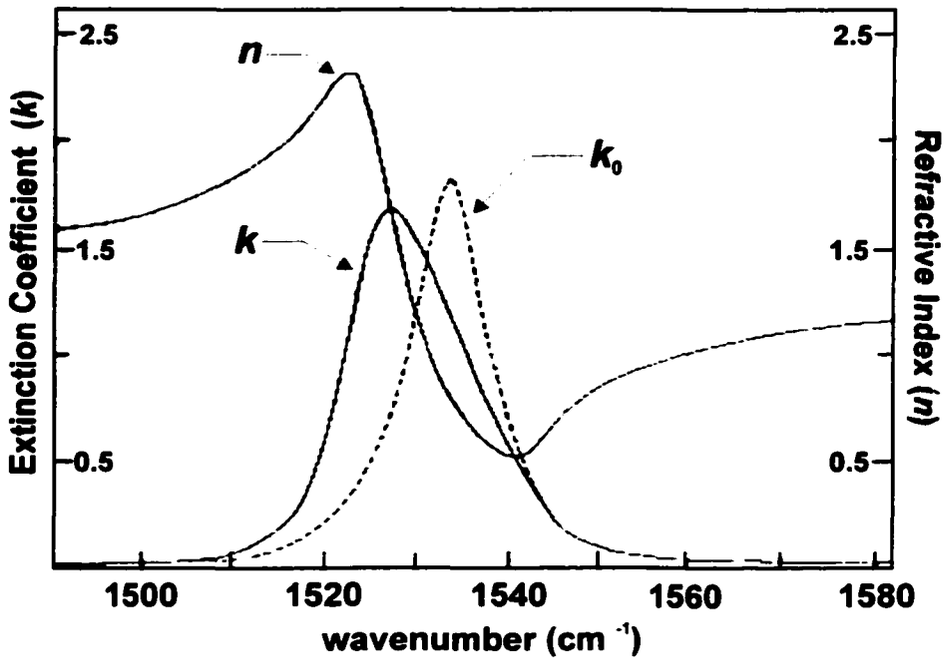

Figure 11. Optical constants from ATR observation on the 1527 cm^{-1} band in liquid C_6F_6: *n*-refractive index, *k* extinction coefficient and k_0 corrected extinction coefficient. Adapted from Fujiyama,T and Crawford B,Jr. Vibrational Intensities.XXI. Some Band Shapes and Intensities in Liquid Hexafluorobenzene. J.Phys.Chem, **1968**, 72,2174-81.

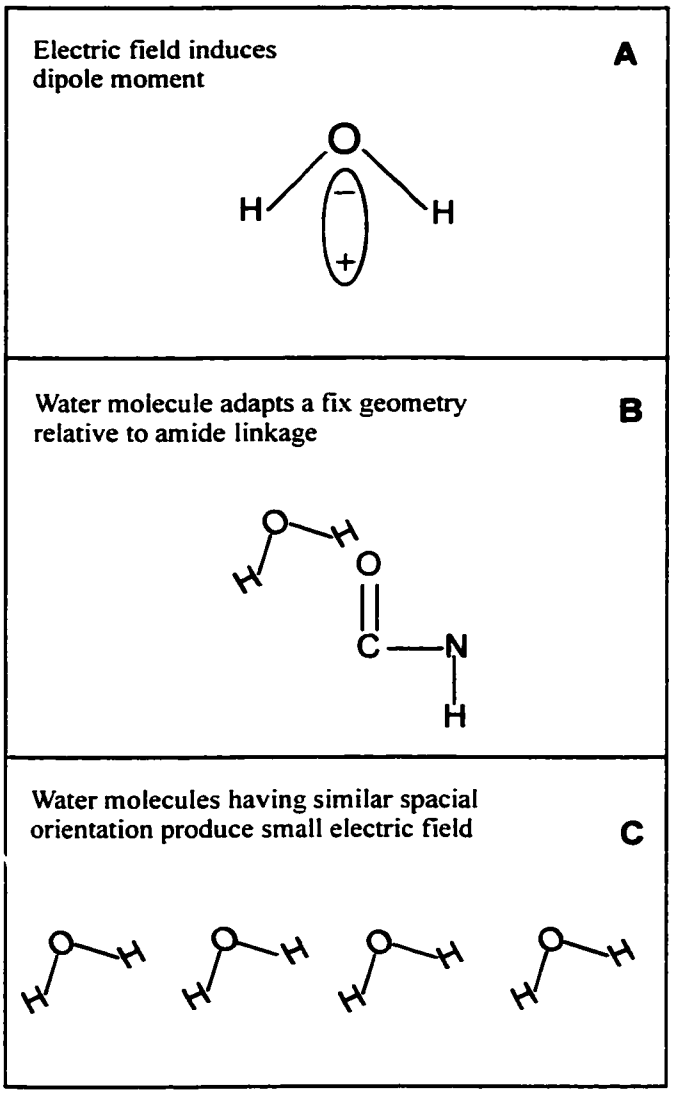

Figure 12. Effect of water on intensities of amide I and amide II bands.

Estimating the Maximum Number of Water Molecules in Sample Pellet

* For this calculation the properties of Human Serum Albumin were used
M.W of of H.S.A is 132,924 g
Number of Amino Acid residues in Protein- 1170

1. Pellet Preparation: 300 mg KBr / 2 mg of Protein.
30 mg of mixtures was used for a pellet. Protein content of a pellet is 0.2 mg.

2. Number of Protein Molecules in a Sample:

$$0.0002\text{g} \times \frac{1\ \text{mole}}{132{,}924\ \text{g}} = 1.5 \times 10^{-9}\ \text{moles of protein}$$

$$1.5 \times 10^{-9}\ \text{moles} \times 6.23 \cdot 10^{23}\ \frac{\text{molecules}}{\text{moles}} = 9.3 \times 10^{14}\ \text{molecules of protein}$$

3. Number of Amino Acids Residues:

$$9.3 \cdot 10^{14}\ \text{molecules} \times 1.17 \cdot 10^{3}\ \frac{\text{residues}}{\text{molecule}} = \mathbf{1.08 \times 10^{18}\ amino\ acid\ residues}$$

4. Number of Water

$$0.0001\text{g} \times \frac{1\ \text{mole}}{18\ \text{g}} = 5.6 \times 10^{-6}\ \text{moles of water}$$

$$5.6 \cdot 10^{-6}\ \text{moles} \times 6.23 \cdot 10^{23}\ \frac{\text{molecules}}{\text{moles}} = \mathbf{3.48 \times 10^{18}\ molecules\ of\ water}$$

The approximate ratio of water molecules to one amino acid in a protein is 4:1

Figure 13. Estimating water content of a sample

Table I. Integrated intensities of amide I and amide II bands of albumin and chymotrypsin

	Peak Heights (absorbance units)		**Peak Heights (a)** (absorbance units)		**Full Width (a,b)** (cm^{-1})		**Integrated Intensity (a,c)**	
Albumin	Amide II	Amide I	Amide II	Amide I	Amide II	Amide I	Amide II	Amide I
Dry Pellet	0.36	0.45	0.35	0.44	98	91	27.28	35.49
Hydrated Pellet	0.42	0.54	0.4	0.53	92	78	27.73	39.91
Solution	0.76	1.3	0.75	1.18	44	53	29.79	63.38
Chymotrypsin								
Dry Pellet	0.26	0.4	0.26	0.38	67	77	15.26	27.23
Hydrated Pellet	0.34	0.58	0.34	0.58	66	63	18.2	34.14
Solution	0.39	0.67	0.37	0.63	68	59	21	34.35

a) obtained by fitting one 50:50 Gauss/ Lorenz band each to the amide I and amide II bands
b) full widths at half heights
c) in absorbance x cm^{-1} units

Chapter 3: The Effect of Hydration on Nucleic Acids Spectra

Abstract: Infrared absorption spectra of DNA and RNA as dry, lyophilized powders in KBr pellets, as hydrated KBr pellets, and in solution phase are reported. The symmetric and antisymmetric stretching vibrations of the phosphate linkage, $\nu_s(PO_2^-)$ and $\nu_{as}(PO_2^-)$ were found to be very sensitive to hydration, as both intensity changes as well as frequency shifts are observed. An increase in water content causes DNA to undergo a structural transition form A-form to B-form. This leads to a conclusion that the frequency shifts are associated mostly with the conformational change, whereas the increase in intensities may be due to an increase of the local dielectric in the vicinity of the polar and solvent exposed phosphate groups. The structure of RNA is less sensitive to hydration, and only the phophodiester stretching vibrations are effected by hydration.

In a previous chapter, a method was described that uses KBr pellets to examine the effect of hydration on proteins. This was accomplished by exposing the KBr pellets which contain the sample to water vapor. This procedure worked well for proteins with different secondary structure motifs, and spectra that represented intermediate states between dry and totally hydrated protein were obtained. In this study the same technique was used to investigate the effects of hydration on the IR spectra of nucleic acids, DNA and RNA.

3.1 Materials and Methods

Calf thymus DNA and baker's yeast RNA were purchased from Sigma Co. and were used without further purification. All samples were stored in accordance with the guidelines specified by the manufacturer and in containers with desiccant. For all solutions distilled water was used as a solvent. All work was conducted at room a temperature (25 °C).

Spectra of dry and hydrated KBr pellets measured on either a Vector 22 or IFS 28/B (Bruker Optics, Billerica, MA) FT-IR spectrometers equipped with DTGS detector at 2 cm^{-1} resolution. One hundred interferograms were co-added for each spectrum of a pellet,and then Fourier transformed using Mertz phase correction procedure and 3-point Blackman –Harris algorithm. The spectrum of pure KBr pellet was used as reference. Pellets were prepared, using a manual pellet press, from about 30 mg of finely ground KBr : DNA (75 : 1 by mass) and KBr : RNA 300:1 (by mass). The diameter of the pellet is 7.48 mm and thickness 0.38 mm. Hydration of the nucleic acids was studied by exposing the pellets at room temperature to a water vapor saturated atmosphere for a well-defined time as described in "Hydration Procedure" section of chapter 2. The hydration was found to be reversible and reproducible.

The absorption spectra of DNA and RNA solutions at 20 mg /mL were measured with 5 μm Teflon spacer and BaF_2 windows. Spectra were collected at 2 cm^{-1} ,and for each spectrum 256 interferograms were averaged. The phase correction and apodization functions used were identical to those applied to KBr pellet spectra. The spectrum of pure water was used as reference. The spectrum of water was iteratively subtracted from DNA or RNA spectrum until the appearance of a straight baseline in a 1750-1900 cm^{-1} region.

All data manipulation was carried out by software developed in-house.

3.2 Hydration of DNA and RNA -Results

Figure 1 shows the IR absorption spectra of dry and hydrated solid DNA, and of an aqueous solution of DNA. Upon hydration of DNA, the PO_2^- antisymmetric stretching vibration, $\nu_{as}(PO_2^-)$, observed at 1238 cm^{-1} in the dry pellet, moves progressively toward lower wavenumber, and reaches 1225 cm^{-1} in aqueous solution.

A similar frequency shift toward lower wavenumber is also observed for the PO_2^- symmetric stretching vibration, $\nu_s(PO_2^-)$. This shift, from 1093 cm^{-1} in a dry sample to 1088 cm^{-1} in solution, is accompanied by a significant increase in peak intensity upon hydration. This increase may be expressed as the ratio of peak intensities of the phosphate vibrations, $\nu_s(PO_2^-)/\nu_{as}(PO_2^-)$, which is about 1.08 for the dry sample. This value increases to 1.5 for the hydrated solid, and reaches about 1.77 for solution spectra. The C-O stretching vibration of the phosphodiester is also effected by the presence of water molecules. Observed at 1062 cm^{-1} in the dry sample, it shifts to 1051 cm^{-1} for the hydrated solid, and to 1054 cm^{-1} in solution.

The increase in water content also modulates the bands in the 1550-1750 cm^{-1} region. These bands are in-plane vibrations of C=O, C=C and C=N groups of the heterocyclic bases. A peak that is characteristic of A-T and G-C base pairing, and sensitive to the conformation of DNA, is observed at 1692 cm^{-1} in the dry samples. This band shifts to 1715 cm^{-1} after hydration. Although this band is partially masked by the very intense O-H deformation band of water in the solution phase spectrum, it can be seen as a shoulder at 1715 cm^{-1} at (Figure 1D).

The observed spectral changes are interpreted in terms of two concurrent effects. One of them is the well-documented conformational change from A- to B-form upon hydration. The other one is a hydration of the phosphate groups that leads to the observed increase in infrared absorption intensities. This change parallels the intensity increase observed for the polar amide I and amide II vibrations in peptides and proteins upon hydration [1]. These effects will be elaborated upon in the Discussion Section below.

The same methodology was used to examine effects of hydration on the spectrum of RNA. RNA has different physical and chemical properties than DNA, and exhibits a different sensitivity to hydration .

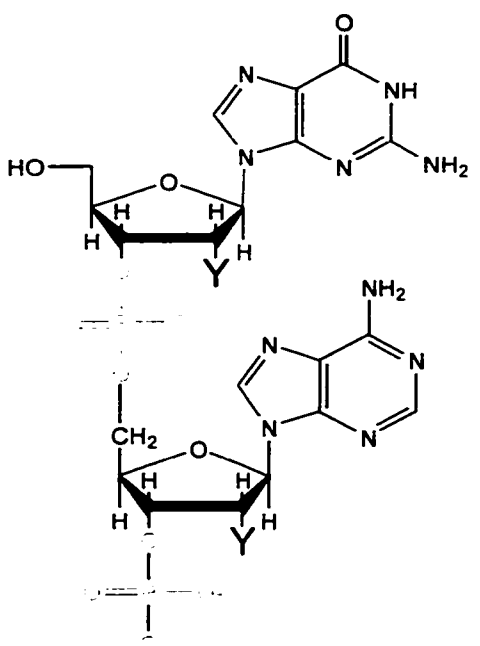

Y=H in deoxyribose, and Y=OH in ribose

First of all, RNA exists only in A-form, since the hydroxyl group attached to the C2' carbon of the ribose ring prevents RNA from transforming to the B form by making it energetically unfavorable [2]. Also because of the C2'-OH group, RNA

is chemically less stable than DNA, and is much more easily degraded by enzymes such as ribonucleases. RNA, in most cases, is single stranded; however RNA can form double-helical structures, by pairing adenine with uracil and guanine with cytosine. The amount of double helical secondary structure depends of the type of RNA (ribosomal, messenger or transfer).

The spectrum of dry RNA in a KBr pellet is shown on Figure 2A. The low frequency region is dominated by the two PO_2^- bands at 1086 and 1238 cm^{-1}. As hydration increases, the contour in the 1000-1165 cm^{-1} region changes, and the intensity of the $\nu_S PO_2^-$ peak increases. This is very similar to what was observed for DNA. For dry RNA, the intensity ratio $\nu_s (PO_2^-) / \nu_{as} (PO_2^-)$ is about 1.4. It increases to about 1.6 for the hydrated solid, and to about 2.0 in solution phase. Although the frequency of the PO_2^- antisymmetric stretching vibration of DNA shifted by 13 cm^{-1} upon hydration, it remains constant in the case of RNA, even after fully hydrating the pellet (Figures 2A-C). However, the appearance of $\nu_{as} (PO_2^-)$ in RNA does effected by hydration, and a small change in the shape of this band can be detected. This is indicated by the appearance of a shoulder at about 1224 cm^{-1} which becomes more pronounced as hydration increases. As in the case of DNA, the bands in the 1550-1750 cm^{-1} region are assigned to C=O, C=N and C=C vibrations of the bases. In this region of the spectrum, much of the band structure remains unchanged, and the slight fluctuation in the intensity of the two major peaks in this region is most likely due to the presence of the water deformation mode in the 1640 cm^{-1} region. The RNA infrared data sug-

gests that hydration mainly effects the polar PO_2^- groups, and that RNA does not undergo any changes in structure.

3.3 Hydration of DNA and RNA - Discussion

The DNA undergoes significant conformational changes as its degree of hydration increases. This is a well-established phenomenon, and the existence of at least two forms of DNA has been known from early x-ray diffraction studies of DNA fibers. In the dehydrated state (when the relative humidity of the environment is around 75 %), DNA assumes a conformation known as A-form. When the relative humidity of the environment is at least 92%, DNA transforms to the B-from, which is considered the native structure [2,3].

There are number of structural differences between the two forms of DNA. Double-stranded, helical B-DNA has an average of 10 bases per helix turn. The helical axis runs through the center of each base pair, and the base pair are stacked nearly perpendicular to the helix axis. In the B-form, the size of the major and minor groves is similar. Double stranded A-form DNA has about 10.9 base pairs per turn, and the base pairs are slightly tilted with respect to the axis by 13^0 to 19^0 degrees. Because of this, the major groove is deep and the minor groove is shallow [4]. Even in relatively low humidity (80 %), DNA is heavily hydrated: there are about 20 water molecules per nucleotide [5]. The hydration is reversible, and transition from one form to another can be achieved by increasing or decreasing the relative humidity of the surroundings.

There are number of reports published in which the A to B transition was investigated by using infrared spectroscopy and infrared linear dichroism: the first

of these date back to the late 50's and yearly 60s [6-10]. There are also a number of review articles available on this subject [11-13]. Most of these studies deal with DNA films or crystals. The phase transition was studied by placing a DNA film in a special cell in which the relative humidity was carefully controlled. The infrared spectra of DNA were then recorded as a function of relative humidity.

The procedure used in these experiments to investigate the hydration effect on polycrystalline DNA utilizes KBr pellets, rather then films: however, our results are identical to those reported in the above-cited studies. The spectrum of DNA shown in Figure 1A corresponds to the spectrum of DNA film recorded by Falk *et al.* at about 50 % relative humidity [9]. This spectrum represent what was labeled "disordered" forms of DNA, characterized by imperfect base stacking. The DNA spectrum shown in Figure 1B is DNA in the A-form, and spectrum 1C represent B-form of DNA. These authors also identified the sequence in which water molecules attach to DNA. According to them, water is first absorbed by the PO_2^- groups, following by the C-O-P and C-O-C groups of the phosphodiester linkage. The last sites of hydration are the DNA bases.

The results reported in this chapter are consistent with this description. After partial hydration of DNA (Figure 1B), no change is observed in the 1450-1750 cm^{-1} region which is sensitive to geometry of base pairs: however, intensity changes and band shifts of the PO_2^- symmetric and antisymmetric stretching vibrations are obvious. Upon further hydration, DNA starts to undergo structural changes (Figure 1C). The 1692 cm^{-1} band moves to higher frequency by 17 cm^{-1}, up to1715 cm^{-1} for the solution spectrum. Thus, initial changes seen in the

DNA spectrum are due to hydration of the exposed polar phosphate groups. Further addition of water induces structural changes in the DNA molecule. In RNA, on the other hand, only the direct hydration of the phosphate groups is observed, and the subsequent conformational change is absent.

This study confirms the hypothesis that was put forth earlier to explain the intensity increase of amide I and amide II bands in proteins. The addition of water can change dielectric environment of a polar group, and increase its infrared absorption intensity quite significantly. In the present study, two competing effects are observed: an increase in hydration of the phosphate groups, followed by hydration of the bases. The first effect causes merely an increase in the absorption intensities of the phosphate vibrations, whereas the second effect causes a conformational change that alters the vibrational spectra more drastically.

Conclusion

For both DNA and RNA, we find the symmetric and antisymmetric stretching vibrations of the PO_2^- group of the phosphate-sugar backbone to be most sensitive to hydration. The uptake of water results in increase in intensity of the ν_s (PO_2^-) vibration in both nucleic acids, and causes a frequency shift of the ν_{as} (PO_2^-) by about 13 cm^{-1} in DNA. In addition to these effects, water induces a structural change in DNA by transforming it from "disordered" form to A-form, and then from A- form to B- form. In the case of RNA, an increased exposure of RNA to water vapor does not result in any changes in secondary structure, and mostly

effects the symmetric PO_2^- stretching intensity of the phosphate-sugar back-bone.

Reference

1. Pevsner, A. ; Diem, M. Infrared Spectroscopic Studies of Major Cellular Componets.Part I. The effect of Hydration on the Proteins. *Appl.Spectrosc.* **2001**, 55 (6), 788-793.

2. Dickerson, R,E. The DNA Helix and How It Is Read. *Sci.Amer.* **1983**,249 (6), 94 -111.

3. Dickerson, R,E.; Drew,H,R.; Conner, BN.; Wing,R,M.; Fratini, A,V.; Kopka, M,L. The Anatomy of A-,B-,and Z-DNA, *Science*, **1982**, 216 ,475-485.

4. Branden, C.; Tooze, J. DNA Structures. *Introduction to Protein Structure*" 2nd ed, Garland, New York,1998; pp212-126.

5. Saenger, W. *Principles of Nucleic Acid Structure*; Springer-Verlag, New York,1984.

6. Sutherland, G,B,B,M.; Tsobui, M . The infared spectrum and molecular configuration of sodium deoxyribonucleater. *Proc.Royal Soc.* **1957**, 239, 446-463.

7. Bradbury, E,M.; Price,W,C.; Wilkinson G,R . Infrared Studies of Molecular Configurations of DNA. *J. Mol. Biol.* **1961**, **3**,301-317.

8. Falk, M.; Hartman, K,A.; Lord, R,C. Hydration of Deoxyrobonucleic Acid.I.Gravimetric Study. *J.Amer.Chem.Soc.***1962**, 84, 3843-3846

9. Falk, M,; Hartman, K,A.; Lord, R,C Hydration of Deoxyrobonucleic Acid.II .An Infrared Study.*J.Amer.Chem.Soc.* **1963**, 85,387-993.

10. Falk,M.;Hartman, K,A.; Lord, R,C. Hydration of Deoxyrobonucleic Acid.III. A Spectroscopic Study of the Effect of Hydration on the Structure of Deoxyribonucleic Acids. *J.Amer.Chem.Soc.*, **1963**, 85, 391-394.

11. Hartman, K,A.; Lord, RC.; Thomas,G,J. Structural Studies. In *Physico-Chemical Properties of Nucleic Acids*" vol 2. Duchesne,J Ed; Academic Press; New York, 1973,Vol 2,pp2-89.

12. Parker, F,S. Nucleic Acids and Related Compounds . *Applications of Infrared, Raman, and Resonance Raman Spectroscopy in Biochemistry*; Plenum Press, New York, 1983; pp349-398.

13. Taillander, E.; Liquier, J.;Taboury, J,A. Infrared Spectral Studies of DNA Conformations. In *Advances in Infrared and Raman Spectroscopy.* vol 12. Clark, R.J.H. and Hester, R.E., Eds; John Wiley & Sons; New York, 1985.pp: 65-114.

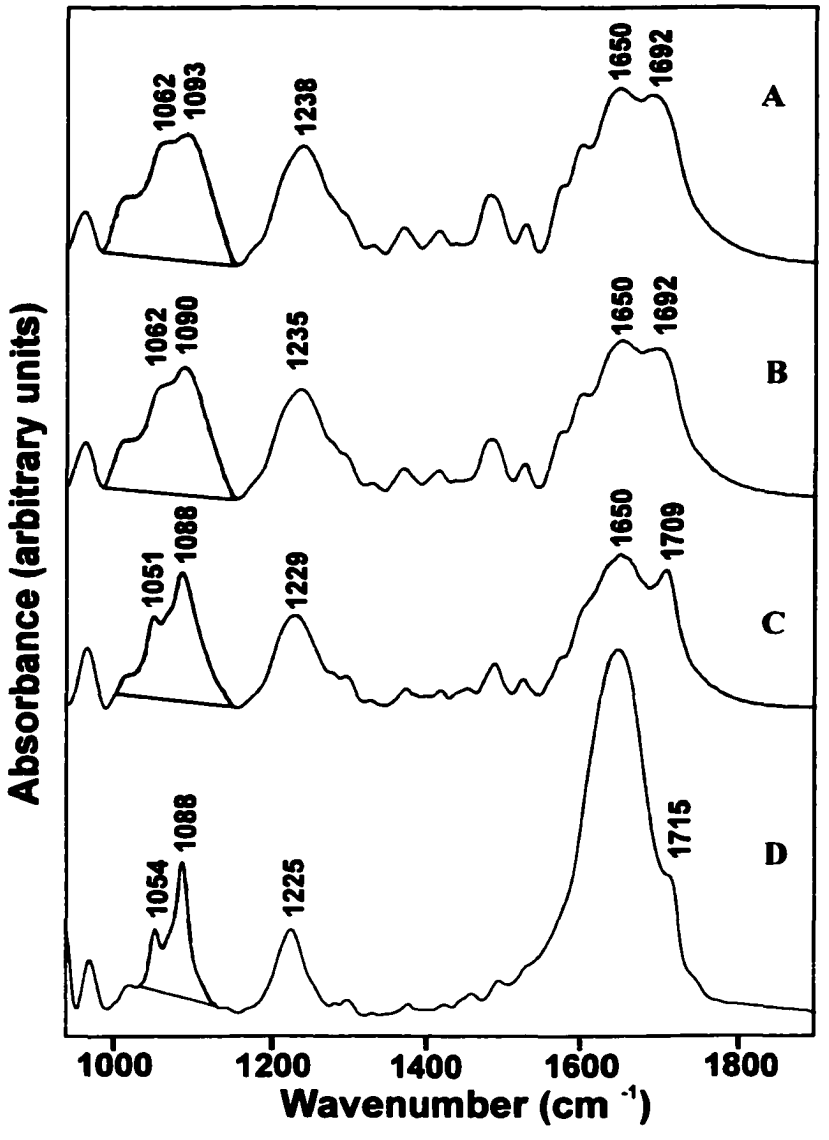

Figure 1. FT-IR absorption spectra of DNA. Trace a) dry DNA in KBr matrix (1:75, by mass); trace b) DNA in KBr matrix (1:75, by mass) after exposure to water vapor for 10 minutes; trace c) DNA in KBr matrix (1:75, by mass) after exposure to water vapor for 20 minutes and trace d) as an aqueous solution (2% w/w) measured in transmission mode. The spectra were not normalized.

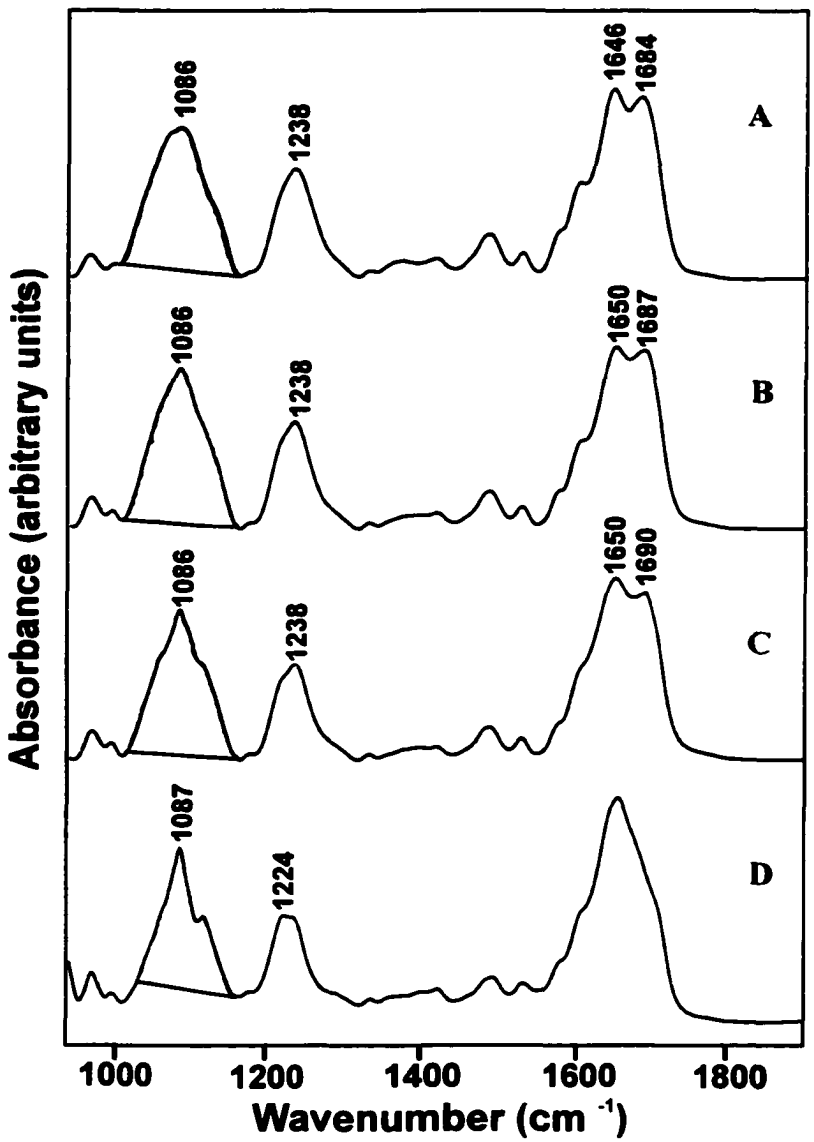

Figure 2. FT-IR absorption spectra of RNA. Trace a) dry RNA in KBr matrix (1:300, by mass); trace b) RNA in KBr matrix (1;300, by mass) after exposure to water vapor for 10 minutes; trace c) RNA in KBr matrix (1: 300 by mass) after exposure of the pellet to water vapor for 20 minutes and d) as an aqueous solution (2% w/w) measured in transmission mode. The spectra were not normalized.

Chapter 4: Hydration of Protein, Nucleic Acid and Phospholipid Films.

Abstract: Infrared absorption spectra of water saturated and continuously dried Protein, DNA, RNA and Phospholipid films as a function of time are reported. It was found that the water in a protein film effects the peak intensity of amide I and amide II bands, as well as the band shape of amide III. For nucleic acids, DNA and RNA, symmetric and antisymmetric stretching vibrations of the phosphate linkage, $\nu_s(PO_2^-)$ and $\nu_{as}(PO_2^-)$, were most effected by a removal of water , as both intensity changes and frequency shifts are observed. The spectrum of a phospholipid film is also sensitive to drying and exhibits changes in the peak intensities as well as the frequencies of both $\nu_s(PO_2^-)$ and $\nu_{as}(PO_2^-)$. The spectral differences between water saturated and dried films were interpreted in terms of both structural changes and the change in local dielectric in the vicinity of the polar and solvent exposed groups. In addition, it is observed that a most significant change in the absorption intensity, frequency and the shape of the water sensitive vibrations occurs within 15 minutes of drying, and further drying only slightly effects intensities of those bands.

In experimental work described in chapter two and three KBr pellets were used to determine the influence of hydration conditions on the infrared spectral patterns observed for proteins and nucleic acids. In the hydration study presented in this chapter, another spectroscopic solid sampling technique, thin film, was used to look at effect of hydration on IR spectra of biomolecules. The films were used in this set of hydration experiments for a number of reasons. First , to confirm the results for alternative technique that changes reported for proteins and nucleic acids upon hydration are genuine and are independent of sample preparation procedure. Secondly, film is a more tradition technique of a vibrational analysis of proteins, nucleic acids and phospholipids, and is thought to be a more relevant model than KBr -embedded sample in approximating a real biological environment.

4.1 Materials and Methods

Human serum albumin, α-Chymotrypsin, calf thymus DNA, baker's yeast RNA and DL-α-Phosphatidylcholine Dimyristoyl were purchased from Sigma Co. and used without further purification.

Protein, nucleic acid and phospholipid films were prepared by casting 30 μL of aqueous solution of a sample onto BaF_2 window and then placing the sample in a vacuum chamber for one hour. The experimental procedure consisted of two steps. First, a film of a given sample was placed in a water vapor-saturated environment for 45 minutes (Figure 1). The film was then removed and immediately placed in the spectrometer for data acquisition. Removal of water from the film was accomplished by providing a continous flow of dry air into the spectrometer's sample chamber. The spectrometer's sample chamber was purged by dry air at the rate of 500 liters per hour (a value that is used for routine data acquisition in this laboratory).

The data was collected on Bruker IF/S 28B FT-IR Spectrometer (Bruker Optics, Billerica, MA) at 2 cm^{-1} resolution. Spectral acquisition started immediately after a sample film was placed into a spectrometer. The spectrometer's software was set up to continuously record a spectrum of the film every 20 seconds for a duration of one hour and seven minutes (total of 200 spectra for each sample). Two interferograms were averaged for each spectrum. Fourier transformation was carried out with Mertz phase correction function and 3-point Blackman –Harris apodization algorithm. The spectra of all

samples examined: albumin, chymotrypsin, collagen, DNA, RNA and phopholipid were not normalized.

4.2 Protein Films -Results

The spectrum of HSA, a predominately α helical protein, as a function of time is shown in Figure 2. There are a number of changes observed after the sample had spent some time in a spectrometer. First, the peak intensity of amide I decreases. Second, the peak intensity of amide II also decreases and the band maximum shifts from 1544 to 1541 cm^{1}. This can be seen in more detail in figure 1B, where a spectrum of a hydrated film (time 0 seconds) and spectrum of a film after 4000 seconds are compared. It is also noticable that amide III band undergoes some changes. First, the intensity of the 1305 cm^{-1} peak decreases and a small change in the band shape of the amide III is observed. The amide III band of a protein is known to be sensitive to conformation and that would suggest that protein's structure may be effected when water is removed from a film. A more dramatic change in the appearance of amide III is observed for chymotrypsin, which is mostly a β sheet protein. The band shape of amide III of hydrated film seen on Figure 3A looks very different from amide III in the spectrum that was recorded a little bit more that one hour later. A small variation in intensity and frequency is observed for band at ca. 1400 cm^{-1}. As for albumin, intensities of both amide I and amide II band are reduced. In addition to that, amide II frequency shifts and the shape of the band change (Figure 3B). The

change in the shape of amide III between hydrated and dried film is particularly evident in a spectrum of collagen seen in Figure 4.

4.3 DNA, RNA and Phospholipid Films-Results

The results for these molecules were group together because all of them have a PO_2^- group, and it is the vibrational modes of this group that seems to be most sensitive to water. Figure 5A and 5B shows a response of DNA to the removal of water. The most noticeable change is a drop in the intensity of symmetric stretching vibration of the PO_2^- group. In a hydrated film the ratio of intensities of the peak at 1089 cm^{-1} to a peak at 1069 cm^{-1} (C-O stretching vibration of phosphodiester linkage) is 1.11 and it is reduced to 0.94 in a spectrum collected at t=4000 seconds. This intensity decrease is also seen for the antisymmetric stretching vibration of PO_2^- but it is not as significant as in the case of $\nu_S PO_2^-$. However, the frequency of $\nu_{AS} PO_2^-$ shifts by 5 cm^{-1} from 1235 cm^{-1} to 1239 cm^{-1}, where as it remains constant for $\nu_S PO_2^-$. For RNA, as for DNA, the intensity of $\nu_S PO_2^-$ significantly decreases, and in addition to that the appearance of this band is dramatically altered in the spectrum of RNA (Figure 5C and 5D). The intensity of antisymmetric vibration seems to lessen by a small amount, and a small frequency shift is observed from 1242 cm^{-1} in hydrated film to 1243 cm^{-1} after drying. The shape of $\nu_{AS} PO_2^-$ in RNA appeared to be significantly effected by the water content of the film.

The spectra of a mixture composed of various ratios of nucleic acids and protein are often used to reconstruct the spectrum of cell. Therefore, in addition

to examining DNA and RNA separately, a mixture made of DNA-RNA-albumin that has 15/15/70 (by weight) composition was examined. The spectrum of this mixture in the frequency region from 900-1300 cm^{-1} behaves very much like a spectrum of pure components (Figure 5E and 5F). A decrease in the peak intensity of $\nu_S PO_2^-$ was observed. A band shape of $\nu_{AS} PO_2^-$ undergoes a considerable change in the appearance and frequency shifts from 1242 cm^{-1} and 1243 cm^{-1}.

In Figures 6 and 7 ,the spectra of a hydrated film and a dried film of phospholipid are compared. Phospholipids, as well as DNA and RNA contain the PO_2^- group and it is evident from the spectra in Figure 6 that the vibrations of this group are most sensitive to a removal of water from the film. First, the intensity of $\nu_S PO_2^-$ drops and the band maximum shifts from 1090 cm^{-1} to 1093 cm^{-1} . The $\nu_{AS} PO_2^-$ band undergoes a very significant modification. The frequency shifts from 1243 cm^{-1} to 1257 cm^{-1} and its shape changes. The band becomes narrower and taller. However, at the same time we did not observed any changes in the frequency and intensity of CH_2 asymmetric stretch and CH_3 symmetric and asymmetric stretching bands of hydrocarbon chains, the vibrational modes that are known to be sensitive to the conformation of a phospholipid (Figure 7).

4.4 Hydration of Films-Results

It was described in "Methods and Materials" section of this chapter that 200 spectra were collected for each sample, and the spectrum of the film was

recorded every 20 seconds for a duration of one hour and seven minutes. The spectra of each sample were examined by monitoring both changes in the 3200-3400 cm^{-1} region where O-H stretching vibration absorbs, and the bands of each sample that is thought by us to be sensitive to hydration. It is apparent that the most dramatic changes in frequencies, intensities and band shapes of water sensitive vibrations of proteins, nucleic acids and phospholipid occurs within 15 minutes after placement of the sample film into the spectrometers sample chamber. Subsequent measurements showed very small variations in position and intensities of water sensitive bands. For all proteins, after 15 minutes, only small decrease in amide I and amide II peak intensities and very minute changes in the shape of the amide III bands were observed. For nucleic acids, the intensity of $\nu_S PO_2^-$ continued to go down. In the case of a phospholipid , the peak intensity of $\nu_S PO_2^-$ did not change after 15 minutes, but a further frequency shift of $\nu_{AS} PO_2^-$ by $2cm^{-1}$ was detected.

4.5 Protein Films-Discussion

At a first glance it may appear that the intensity decrease of amide I and amide II vibrations may simply be due to the diminishing contribution of the liquid water O-H deformation band observed at ca. 1635 cm^{-1}. To confirm this, the dehydration process was modeled by adding a scaled spectrum of liquid water to the spectrum of most dried samples (a spectrum obtained at t=4000 sec). It is the same mathematical procedure as used to model hydration of pellet and is described in details in section 1.3. Indeed, the addition of water caused the

increase in intensity of both amide I and amide II bands. However for all proteins, albumin, chymotrypsin and collagen, the combined spectrum of water plus dried film did not resemble a spectrum of hydrated film, and our modeling did not reproduce a band shape or frequency shift of amide II seen in both proteins. This result, together with the fact that both proteins exhibit a noticeable change in amide III band shape, leads to a conclusion that proteins undergo a slight structural modification when water is removed from a film. This agrees with earlier studies on proteins were KBr pellets were used to examine the effect of hydration on a spectra of protein [1]. Using KBr pellets, it was determined that any variation in the amount of bound water results in change of band shape of amide III and the intensities of amide I and amade II bands and the identical results are seen using film. However, the changes in the band shape of amide III in the spectra of all three proteins are more pronounced compared to the changes in amide III observed when the hydration of same proteins was studied using KBr pellets. This can easily be explained. Water that is taken by KBr disc degrades the quality of a pellet and consequently the quality of spectrum, where as water in a film has virtually no effect on the quality of data collected.

The spectra of albumin, chymotrypsin and collagen are *raw spectra* and *were not normalized*. The bands that are mark with asterisk on figures 2,3,and 4, namely 1452 cm^{-1} band in albumin,1398 cm^{-1} in chymotrypsin and 1082 cm^{-1} band in collagen were used before to normalize the spectra of dry and hydrated

pellets. These are virtually uneffected by hydration. These particular results confirm the validity of the pellets experiments described in chapter 2.

4.6 DNA and RNA Films-Discussion

The decrease in $\nu_S\ PO_2^-$ intensity and the frequency shift of $\nu_{AS}PO_2^-$ agrees with results obtained from examining the hydration of nucleic acids using KBr pellets and with earlier work on DNA films by others [2-5]. The changes seen in DNA spectrum are explained in terms of DNA undergoing a structural transition from B-from (a highly hydrated form) to A-form (less hydrated form). The substantial variation in the $\nu_S\ PO_2$ peak intensity can be explained by hypothesis that was put forth in a previous chapter. The intensity seen upon dehydration may be due to decease in dielectric constant in the vicinity of the polar and solvent exposed phosphate group. This explanation is also applicable to RNA. RNA only exists in one form – A-form. Thus, water can not induce any structural transition, yet in RNA as in DNA we observe significant variation in $\nu_S\ PO_2^-$ intensity. Water however, may be responsible for changing dielectric constant around phosphate group which in turn effects intensity of $\nu_S PO_2^-$.

4.7 Phospholipid Films-Discussion

Phosholipids have been extensively studied by a number of techniques, including Raman as well as IR spectroscopy. The vibrational assignment of the peaks is well known. The dependence of IR spectrum of phospholipids on the changes of environment, such as temperature and pressure, are also well documented in

literature [6,7]. It is know that phospholipids can undergo a transition from "gel" to "liquid crystal" phase by varying the temperature or pressure in a system. The bands that are sensitive to the transition from one phase to another are the symmetric and asymmetric CH_3 stretching vibrations and CH_2 asymmetric stretching vibrations of fatty acids chains in the 2800-3100 cm^{-1} region. When parameters such as pressure and temperature are altered, the intensity and frequency shifts of those bands are observed. Initially it was speculated that the change in the spectrum of the phospholipid seen in Figure 6 is due to phospholipid undergoing some structural change. However, a more detailed analysis of spectra reveals that frequency and intensity of CH_3 and CH_2 bands remained unaltered when water is removed from phospholipid film (Figure 7). Thus, water may effect the orientation and dielectric environment of the polar phosphate group leaving the rest of the phospholipid molecules unchanged. This may explain the decrease of νPO_2^- peak intensity and frequency shifts of $\nu_{AS}\, PO_2^-$ to higher wavenumbers and unaltered band shapes and frequencies of CH_2 and CH_3 vibrations.

4.8 Hydration of Films-Discussion

The experimental data suggests that removal of water proceeds in two steps. Liquid water that is loosely bound on surface of the film is removed first. This does agree with our observations because the most significant change in the curvature of water sensitive bands is seen during the first 15 minutes. In the second phase, bound water is removed from structure of proteins, nucleic acids

or phospholipid, and this process probably continues until a system reaches an equilibrium, since after 15 minutes we still see variations in the intensities of water sensitive bands.

Conclusion

This set of experiments where films of biomolecules instead of KBr pellets were used is a very important part of a hydration work presented in here. First, it confirms that amount of bound water effects the intensity of amide I and II , as well as band shape of amide III band for proteins , and intensity and frequency of $\nu_S PO_2^-$ and $\nu_{AS} PO_2^-$ bands in nucleic acid and phospholipids. Secondly, this study demonstrates that the same hydration result can be obtained regardless of the sampling procedure, used and confirms that results observed for pellets are genuine and not an artifact.

References

1. Pevsner, A.; Diem, M. Infrared Spectroscopic Studies of Major Cellular Components. Part.I.The effect of Hydration on the Spectra of Proteins. *Appl.Spectrosc.* **2001,** 55 (6),788 – 793.

2. Pevsner, A.; Diem, M. Infrared Spectroscopic Studies of Major Cellular Components.Part.II. The effect of Hydration on the Spectra of Nucleic Acids. *Appl.Spectrosc.* **2001,** 55(6), 1502-1511.

3. Sutherland, G,B,B,M.; Tsobui, M . The infared spectrum and molecular configuration of sodium deoxyribonucleater. *Proc.Royal Soc.* **1957**, 239, 446-463.

4. Bradbury, E,M.; Price,W,C.; Wilkinson G,R . Infrared Studies of Molecular Configurations of DNA. *J. Mol. Biol.* **1961**, **3**,301-317.

5. Falk, M,; Hartman, K,A.; Lord, R,C. Hydration of Deoxyrobonucleic Acid.II.An Infrared Study.*J.Amer.Chem.Soc.* **1963**, 85,387-993.

6. Parker, F,S. Model Membranes, Biomembranes, and Lipid Containing Systems. In *Applications of Infrared, Raman, and Resonance Raman Spectroscopy in Biochemistry* Plenum Press; New York, 1983; pp381-401.

7. Casal, H.;Matsch, H,H. Polymorphic Phase Behaivor of Phospholipid Membranes studied by Infrared Spectroscopy. *Biochim. Biophys.Acta.* **1984**, 779, 381-401.

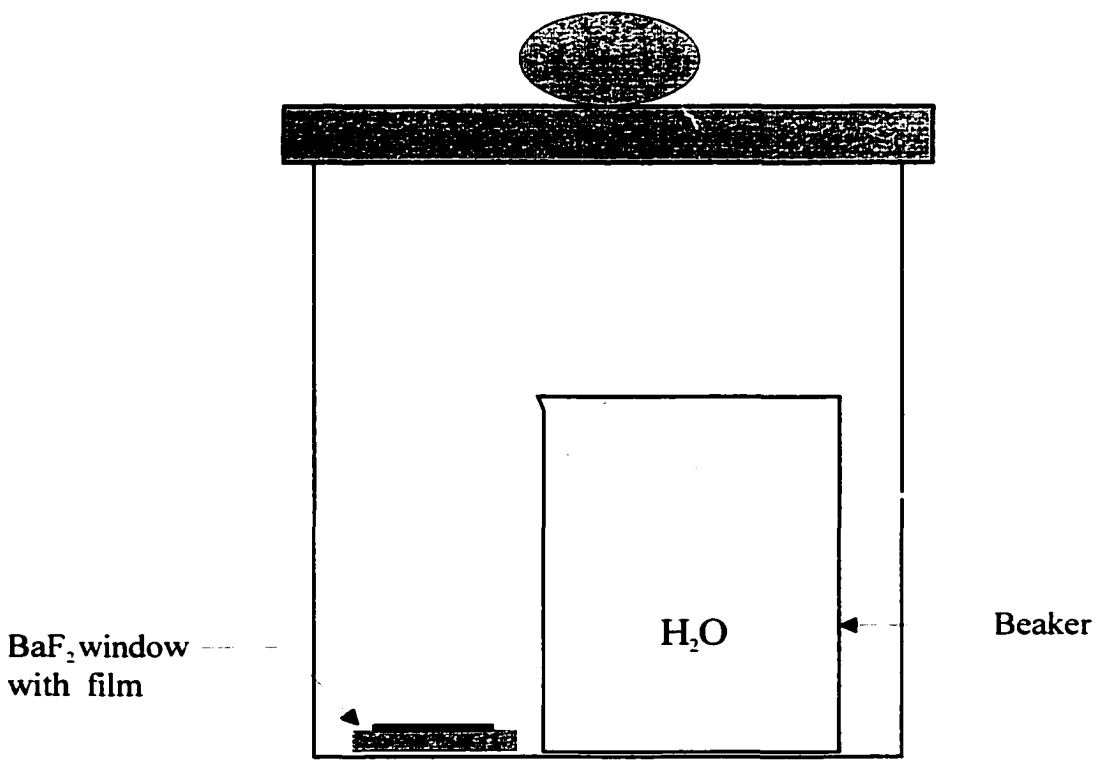

Figure 1. Setup of the hydration experiment using film sampling method. The sample holder with KBr disc is placed on top of the beaker with water that is inclosed in an air-tide vessel .

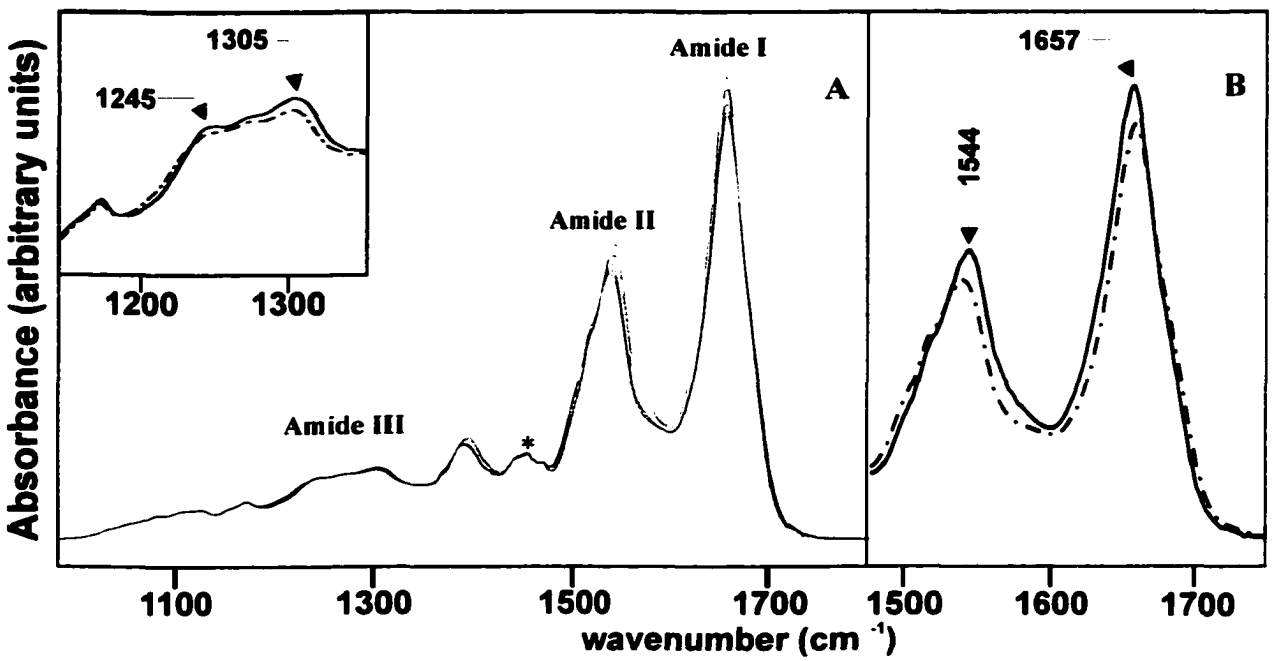

Figure 2. Unormalized FT-IR absorption spectra of albumin film. Trace A) collected over a period of 4000 seconds; trace B) expanded amide I/amide II region of albumin film collected at 0 seconds (solid trace) and at 4000 seconds (dashed trace). The asterisk indicates a band at 1452 cm^{-1}.

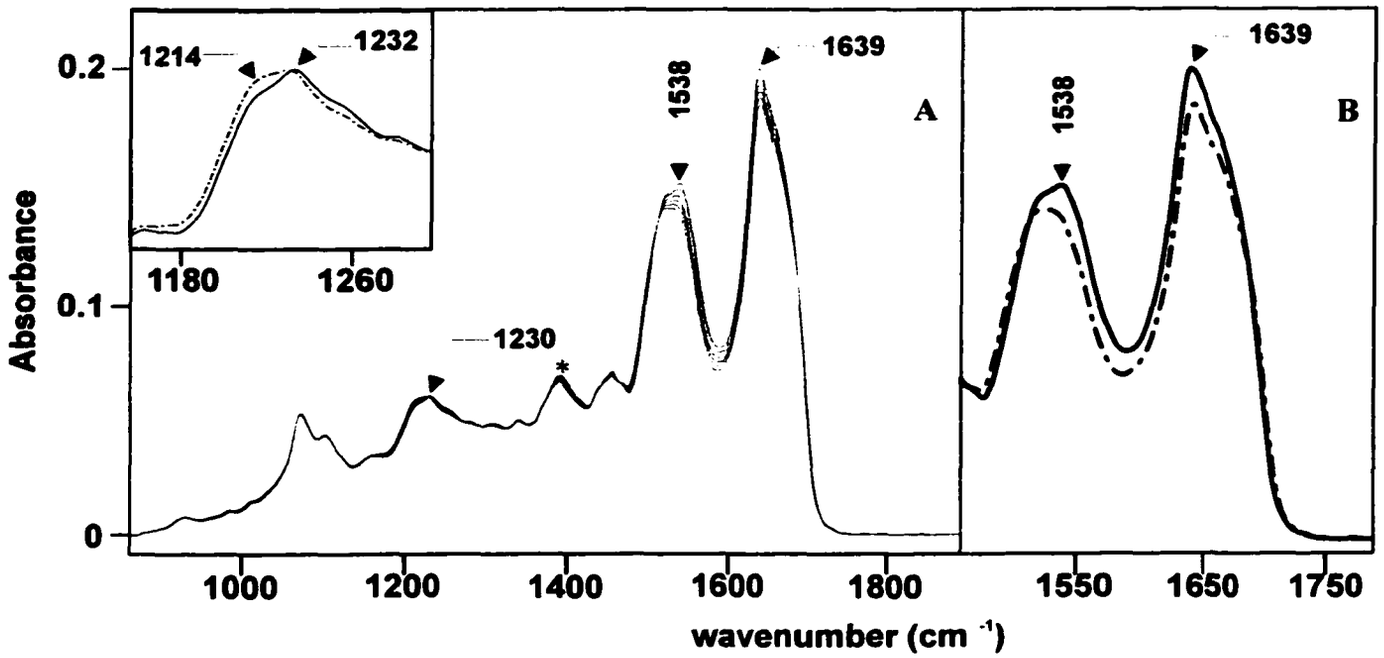

Figure 3. Unormalized FT-IR absorption spectra of chymotrypsin film. Trace A) collected over a period of 4000 seconds; trace B) expanded amide I/amide II region of albumin film collected at 0 seconds (solid trace) and at 4000 seconds (dashed trace). The asterick indicated a band at 1398 cm^{-1} .

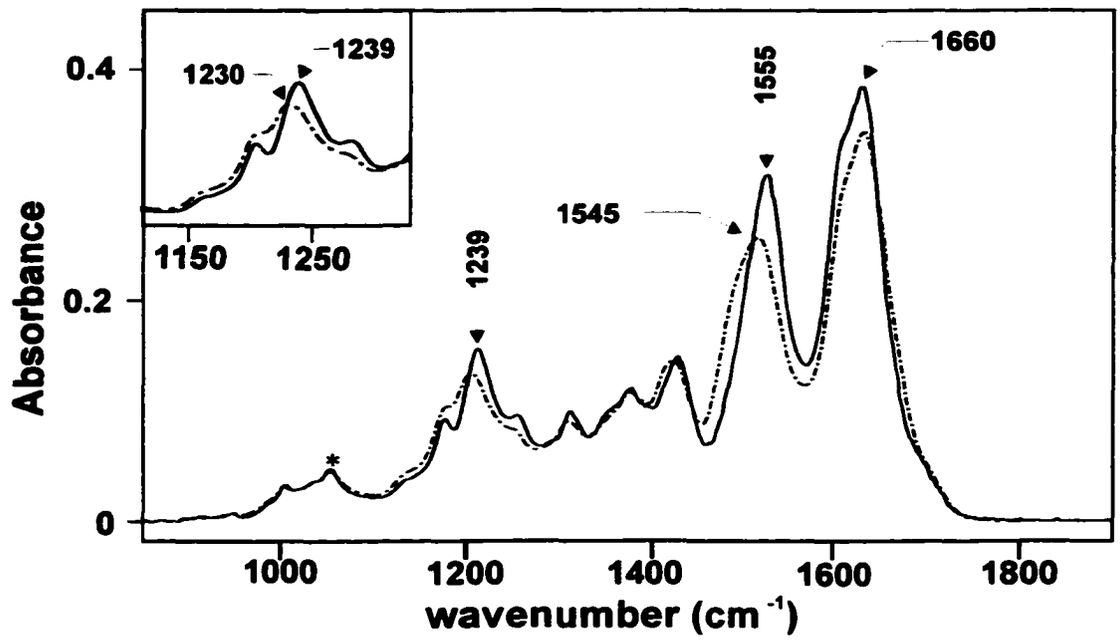

Figure 4. Unormalized FT-IR absorption spectra of collagen film collected at t= 0 seconds (solid trace) and t=4000 seconds (dashed trace).
* indicates a band at 1082 cm^{-1} .

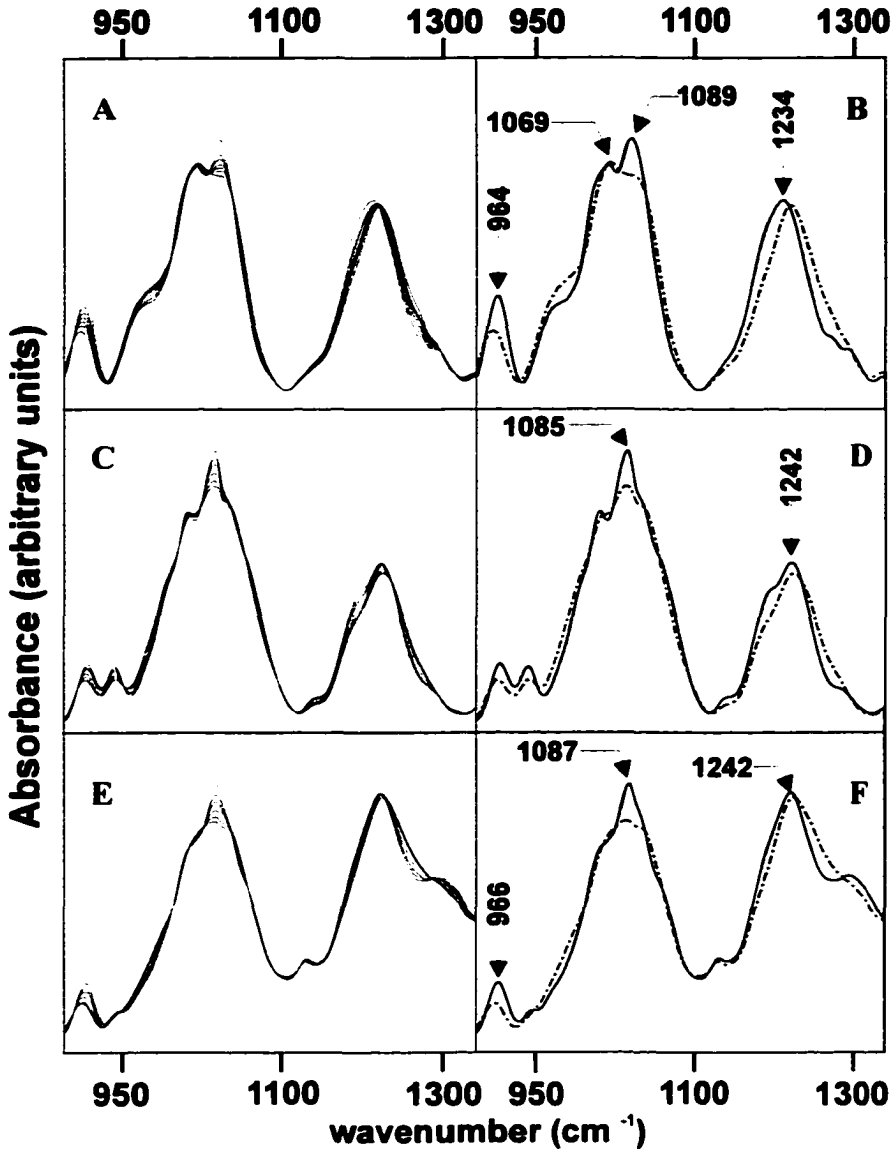

Figure 5. Unormalized FT-IR absorption spectra in 900 -1300 cm^{-1} region of A) DNA film collected over a period of 4000 seconds B) DNA film collected at 0 seconds (solid trace) and at 4000 seconds (dashed trace) C) RNA film collected over a period of 4000 seconds D) RNA film collected at 0 seconds (solid trace) and at 4000 seconds (dashed trace) E) DNA-RNA-Protein film (15/15/70 by weight) collected over a period of 4000 seconds F) DNA-RNA-Protein film collected at 0 seconds (solid trace) and at 4000 seconds (dashed trace).

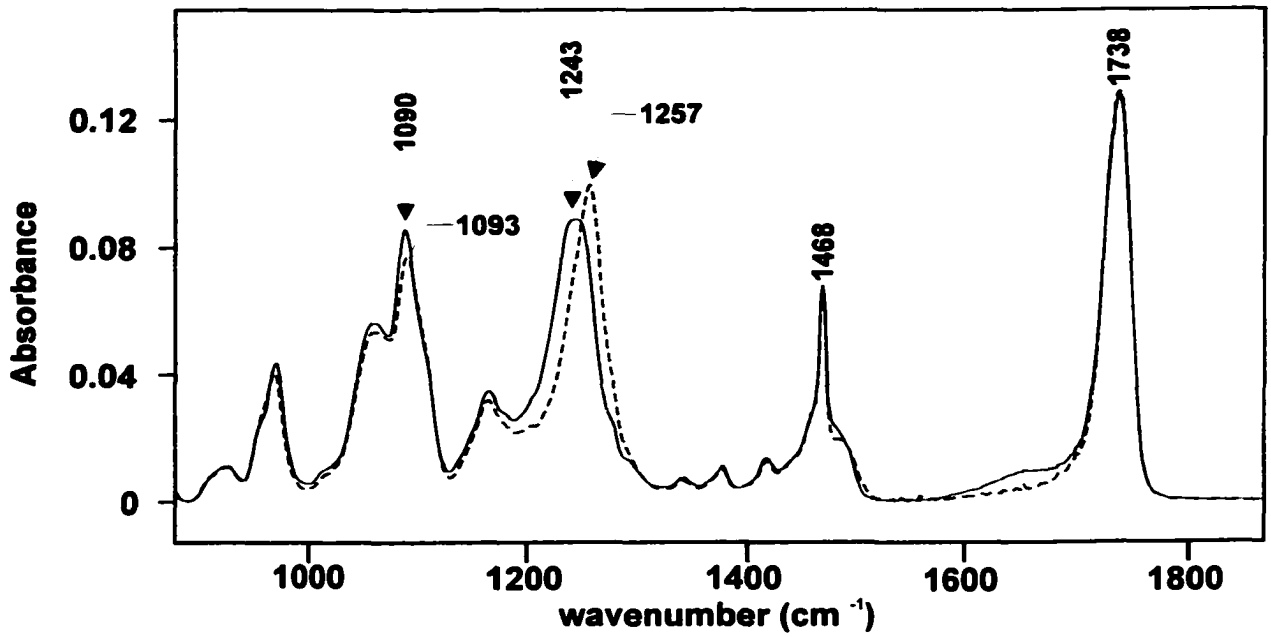

Figure 6. Unormalized FT-IR absorption spectra of Phosphatidylcholine film collected at 0 seconds (solid trace) and 4000 seconds (dashed trace).

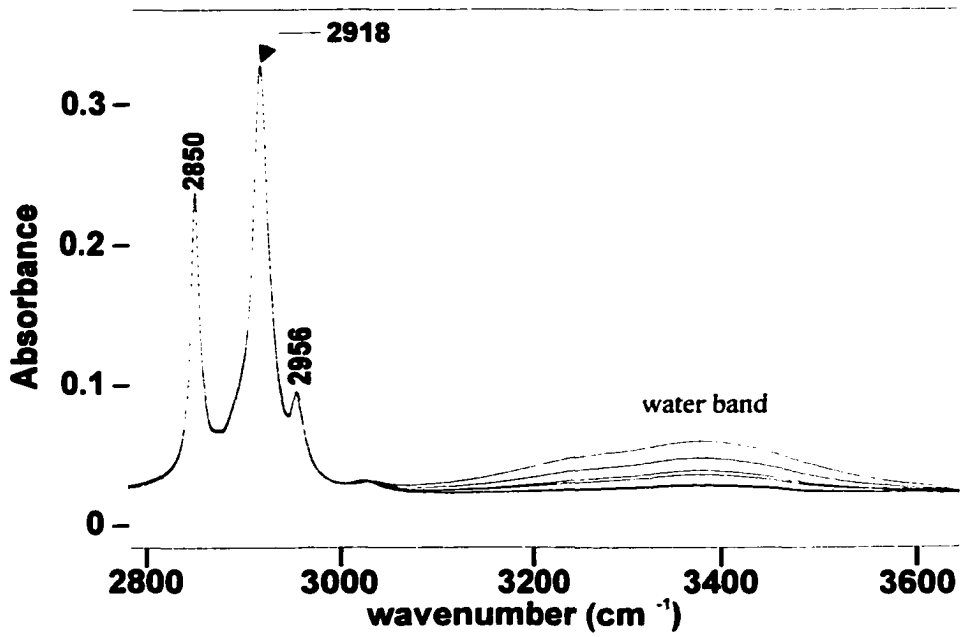

Figure 7. Unormalized FT-IR absorption spectra of Phosphatidylcholine film in 2800-3600 cm^{-1} frequency region collected over a period of 4000 seconds.

Chapter 5: Attenuated Total Reflection (ATR) and Comparison of ATR and Transmission Spectra of Proteins and Nucleic Acids

Abstract: The spectra of aqueous protein and nucleic acid solutions collected in a transmission mode were compared with the spectra of the same solutions that were collected using an ATR accessory. For proteins, a reversal of the amide I to amide II intensity ratio was observed for solutions measured using ATR method. For nucleic acids, DNA and RNA, the spectra collected in transmission and ATR mode were identical in the frequency region between 900-1300 cm^{-1}. The spectra of hydrated and dry collagen acquired using three different infrared spectroscopic techniques, KBr pellet, film and ATR, were also compared.

When examining hydration effect, the spectra of dry and hydrated pellet were compared with the spectra of aqueous solutions. All spectra of solution presented so far were measured in transmission mode. Collecting transmission spectra of aqueous samples is a difficult task. There is a much more convenient method available for obtaining the infrared spectra of solution, Attenuated Total reflection (ATR). This chapter details the study of aqueous solutions of DNA, RNA and protein using Attenuated Total Reflection (ATR) technique. The experiments presented here had two fold purpose: a) to test the hypothesis that infrared spectra acquired with ATR accessory are similar to infrared spectra of solutions collected in transmission mode and b) to confirm results obtained from hydration studies described in previous chapters.

5.1 ATR Theory

Figure 1 (A,B) depicts a schematic of the Pike™ ATR accessory used in these experiments. The main component of the ATR accessory is a trapezoidal ZnSe crystal mounted in a metal casing. ZnSe is an ideal ATR crystal because of its relatively high refractive index (2.4 at 1000cm^{-1}) and low solubility. The FT-ATR

spectroscopy utilizes the physical phenomenon of total internal reflection. When an infrared beam enters a ZnSe crystal at an angle that is equal to or larger than a critical angle, total internal reflection is observed and a beam travels within a crystal without any loss of intensity. However, a small portion of the beam, known as the evanescent wave, penetrates beyond a physical boundary of the ATR crystal surface. In a typical ATR experiment, the evanescent radiation is absorbed by a sample that is in contact with the crystal surface, producing an infrared absorption spectrum. The penetration depth of the infrared beam in the ATR crystal can be determined from the equation:

$$DP=1/\,2\pi\ \bar{\nu}\ N_C\ (\sin^2\Theta - N_{SC})^{1/2}$$

where DP-depth of penetration

$\bar{\nu}$ =wavenumber of incident radiation

N_C-refractive index of a crystal

Θ-angle of incidence

$N_{SC}=N_{SAMPLE}/N_{CRYSTAL}$

The penetration depth of the infrared beam in ZnSe crystal at the angle of incidence 45 and 1000 cm^{-1} is about 1.6 μ for a sample with refractive index 1.4. The small penetration depth of the evanescent wave greatly diminishes the contribution of liquid water to the overall sample spectrum. Furthermore, the spectrum of water can be subtracted using standard spectroscopic software. The main advantage of ATR is the ease with which infrared spectra of aqueous

solutions can be collected. The aqueous sample is simply pipetted onto a surface of the crystal and the spectra can be rapidly collected. The transmission measurements require construction of the liquid cell that consists of 5 μm thick teflon spacer that is sandwiched between two BaF_2 or CaF_2 windows (Figure 2). The spacers of this size are difficult to purchase commercially, and therefore each spacer has to be cut manually from a large piece of teflon material. Cutting and assembling the liquid sampling cell with a spacer of this size is a difficult task. There is another drawback of a liquid cell. It is almost impossible to reproduce the same path lengths from one cell to another, and therefore ATR is a more convenient way to analyze solutions.

The first thorough description of theoretical and experimental aspects of ATR was given by Harrick [18] in the late 1960's. In spite of its obvious advantages over FTIR transmission spectroscopy few studies have focused on biological molecules. However, ATR provides information about the molecular structure of the sample at the interface rather than from entire sample thickness or bulk . The highly ionic ZnSe crystal may modify the molecular structure of DNA, RNA and proteins at the crystal's interface possibly resulting in difference between spectra recorded with an ATR accessory and those recorded in transmission mode (Figure 2) . Whether this statement is valid can only be answered by comparing the spectra of sample in both transmission and ATR mode.

5.2 Methods and Materials

Human serum albumin,type III collagen, calf thymus DNA and baker's yeast RNA were purchased form Sigma Chemicals, Inc., in form of lyophilized powders and used without further purification. All experimental procedures including sample preparation and data collection were conducted at room temperature (25 ^{0}C). All solutions were prepared by dissolving a given sample in distilled water.

The spectra of solutions were collected using an IFS 28/B (Bruker Optics, Billerica, MA) FT-IR spectrometer using DTGS detector. The absorption spectra of human serum albumin,DNA and RNA in aqueous solution at 20 mg/mL were recorded in transmission mode and measured using a 5 μm Teflon spacer and two BaF_2 windows. The absorption spectrum of water collected under the same conditions was used as the reference spectrum. ATR measurements of human serum albumin, DNA and RNA solutions at concentrations of 60 mg/mL, 20 mg/mL and 20mg/mL , respectively. Measurements were carried out using a horizontal, multi-reflection ZnSe crystal (PIKE, Inc.). The ATR accessory has a 45 degree angle of incidence and the ATR crystal size is 7×1 cm. The ATR spectrum of pure water was used as the reference spectrum. The criterion for subtraction of water from the ATR and transmission spectra of aqueous solutions of proteins and nucleic acids was a straight baseline between 1750-1900 cm^{-1}. For each spectrum 256 scans were co-added at resolution of 2 cm^{-1}. The interferogram was Fourier transformed using Mertz phase correction and 3-point Blackman–Harris apodization function. Spectra were then converted to a platform

independent format used in this laboratory. All subsequent data manipulation was carried out by software developed in-house.

The ATR spectra of collagen "gel" at different stages of water saturation were acquired on MIDAC Series M (Midac, Inc, Costa Mesa, CA) FT-IR spectrometer equipped with MCT detector, and were collected in the following manner. First, 5 mg of collagen fiber was place into a small cuvette containing 1 mL of water (0.5% w/w) and was allowed to stand at room temperature (25 ^{o}C) for approximately an hour. Collagen in water forms an extremely viscous gel-like substance. In this study collagen gel was assumed to be most hydrated form of this protein. The gel was spread with a micro spatula over the entire surface of ATR crystal (the same crystal used for ATR measurement of aqueous solutions) and data collection commenced immediately thereafter. The spectra were recorded continuously every 10 seconds for a duration of 6 minutes while the water was evaporating from the collagen gel. A reference spectrum for this data set was recorded on a sample free ZnSe crystal. For each spectrum 10 scans were co-added at 2 cm^{-1} resolution. Fourier transform of the interferogram was performed using Mertz phase correction and medium Norton-Beer apodization function. The spectra were then transferred to a personal computer and manipulated using software written in house.

5.3 ATR vs. Transmission-Results and Discussion.

Figures 3 shows the spectrum of albumin collected in transmission mode and using the ATR accessory. These two spectra demonstrate an intensity

reversal in the structurally sensitive region of the protein spectrum, 1600-1800 cm^{-1}. The amide I /amide II ratio for albumin in transmission spectrum is 1.15 . For ATR spectrum the intensity ratio is 0.80. However, the amide I band of a protein, and the water O-H deformation mode absorb in the same region, *ca.*1650 cm^{-1} and the reversal the intensity ratio seen in a spectrum of ATR may be due to inadequate subtraction of the liquid water from the spectrum of aqueous protein. The subtraction algorithm is,

protein solution ATR spectrum – constant × ATR water spectrum

The *constant* in the subtraction procedure was chosen to produce a straight baseline in 1700-1900 cm^{-1} region. This is the same guideline that was used when transmission spectrum of aqueous protein was compensated for water. Four different subtraction constant were considered ranging from 0.96 to 1, yet the ATR and transmission spectra did not resemble each other (Figure 4). Others observed the same reversal ratio for ATR measurements on whole blood, and aqueous albumin [2-4]. The spectrum of dry albumin film collected via ATR was also examined, and amide I/amide II ratio for this sample is greater than unity (Figure 5). The amidel/amide II ratio reversal for this particular protein is a consequence of inability to properly subtract water ATR spectrum from the spectrum of protein solution.

The depth of penetration of infrared beam is dependent on the ratio of refractive indices of a crystal and a sample. When a protein solution is pippeted into an ATR accessory it is immediately adsorbed onto the highly ionic ZnSe crystal surface forming a dense protein layer (Figure 2B). The fact that albumin is

strongly attaches to the crystal's surface is an evidence of favorable interactions between protein and crystal's material. The protein layer may well have a different refractive index then water, and refractive index of sample effects the penetration depth of the beam. Consequently, the penetration depth of infrared beam in the 1600-1800 cm^1 region for the protein solution and water will not be the same making it impossible to properly subtract the spectrum of water from the spectrum of aqueous solution of a protein. There is also another possible explanation. There may exist a water gradient within adsorbed protein layer, which also could be a potential source. At present time no definite explanation can be proposed, and hypothesis described here can only be verify through additional study which would need to involved the use of ATR accessory with variable angle of incidence and various types of crystal materials such as ZnSe, Ge and KRS-5.

The transmission and ATR spectra of DNA and RNA were also compared. Figure 6 shows that the transmission and ATR spectra of both nucleic acids are identical in 900 –1300 cm^{-1} region which is dominated by $\nu_S PO_2^-$ and $\nu_{aS} PO_2^-$ vibrations. These results also confirm the hydration work with nucleic acids pellets and films presented in previous chapters.

In Figure 7, the amide III band of hydrated and dehydrated collagen obtained from ATR time dependent study is compared with amide III of hydrated and dry KBr pellets and hydrated and dehydrated collagen films. Regardless of sampling technique employed for data collection, the amide III region of hydrated collagen looks identical whether it is ATR spectrum, spectrum of hydrated

collagen in KBr disc or hydrated film. The most intense peak of amide III "triad" in hydrated protein is observed at 1238 cm^{1} . The ratio of two neighboring peaks at 1205 cm^{-1} and 1281 cm^{-1} is 1.04. In dry sample this ratio is 1.19 and the most intense band shifts to 1232 cm^{-1}.

Conclusion

The reversal of amidel/amide II ratio was observed when transmission and ATR spectra of aqueous albumin solution where compared, and two possible explanations for this observation where proposed. DNA and RNA ATR and transmission spectra in 900-1300 cm^{-1} range found to be identical. In addition, ATR hydration results for collagen completely agree with hydration work where pellets and films were used.

Attenuated Total Reflection is convenient infrared sampling method for collecting spectra of solutions. However, additional work ATR studies will with proteins and nucleic acids solution will need to conducted to insure the compatibility of results obtained from regular transmission and ATR measurements

Reference

1. Harrick,N.J. *Internal Reflection Spectroscopy*.John Wiley & Sons, New York, 1967.

2. Heise, H,M; Marbach, R; Janatsch, G: Kruse-Jarres,G.D. Multivariate Determination of Glucose in Whole Blood by Attenuated Total reflection Infrared Spectroscopy. *Anal.Chem.*, **61**, 2009-2015 (1989).

3. Janatsch, G; Kruse-Jarres,J,D; Marbach,R; Heise,H,H . Multivariate Calibration Assay in Clinical Chemistry Using Attenuated Total Reflection Infrared Spectra of Human Blood Plasma. *Anal.Chem.*, **61**, 2016 (1989)

4. Heise,H,M; Marbach, R;Koschinski,T ;Gries, F,A. Multicomponent Assay for Blood Substrates in Human Plasma by Mid-Infrared Spectroscopy and its evaluation for Clinical Analysis. *Appl.Spectrosc.*, **48**(1), 85-95 (1994).

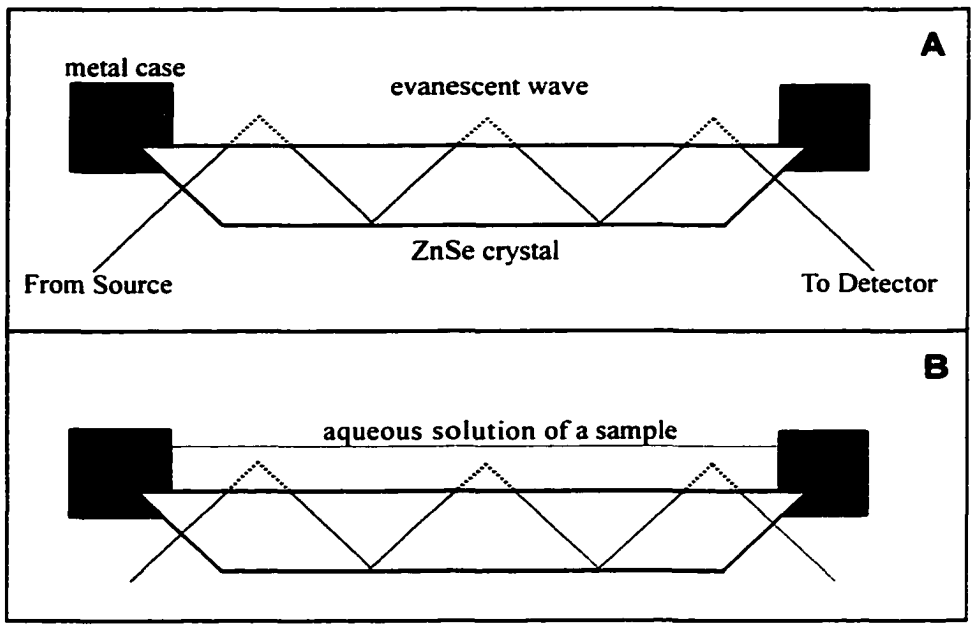

Figure 1. A diagram of ATR accessory.

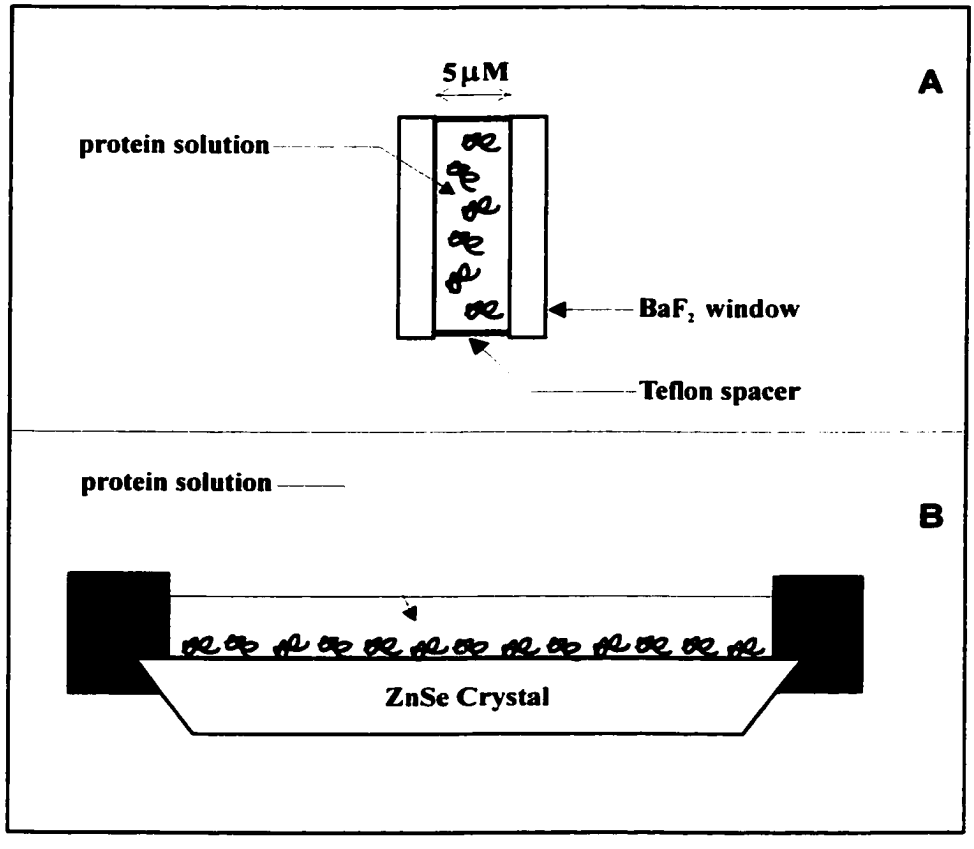

Figure 2. A) transmission measurements B) ATR measurements.

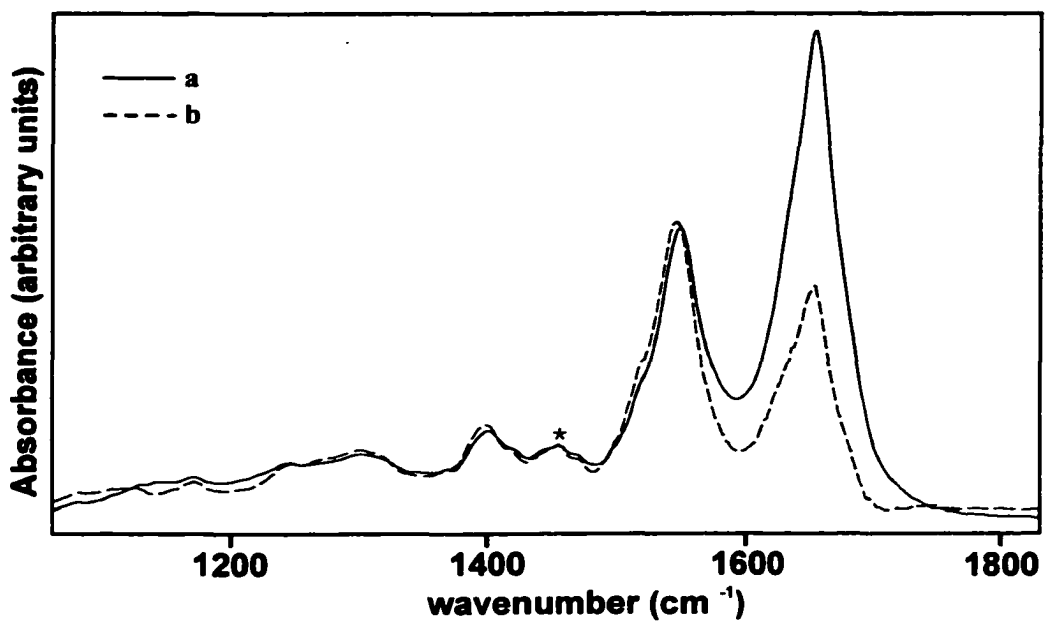

Figure 3. Trace a) FT-IR absorption spectrum of an aqueous solution of albumin (2% w/w) measured in transmission mode (5 micron pathlength, BaF_2 windows); trace b) FT-ATR absorption of an aqueous solution of albumin (6% w/w), measured via a multireflection ATR method on ZnSe. * The spectra were normalized at 1452 cm^{-1}.

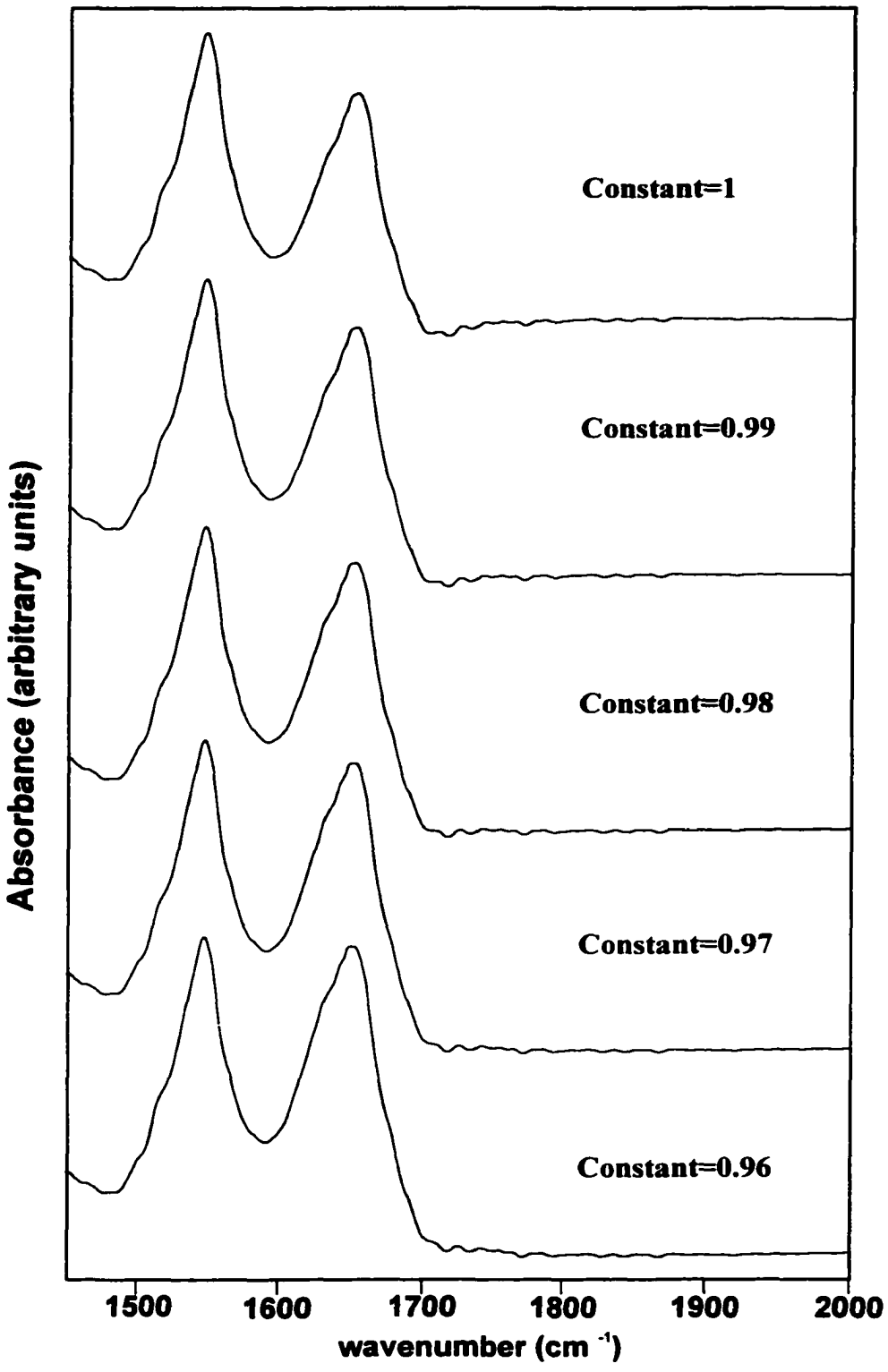

Figure 4. Subtraction of water spectrum from the spectrum of aqueous protein solution using equation **protein solution ATR spectrum - constant * water ATR spectrum**

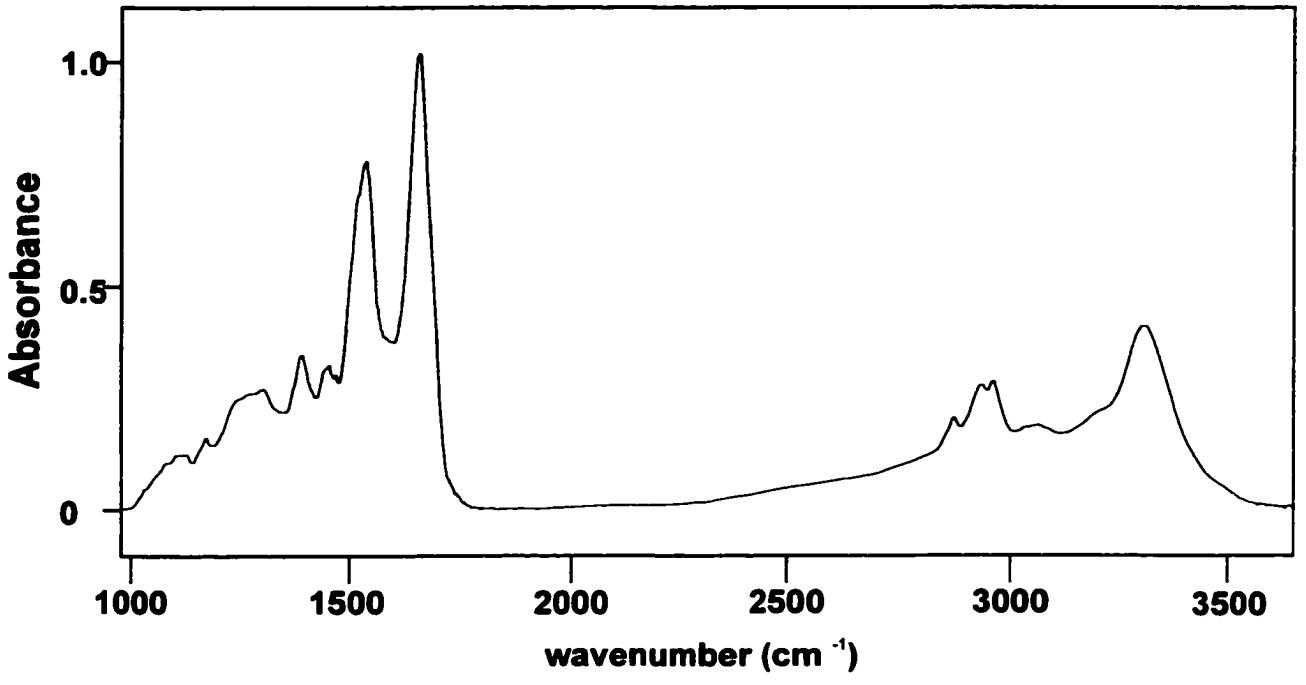

Figure 5. FT-ATR spectrum of dry albumin film measured via a multireflection ATR method on ZnSe.

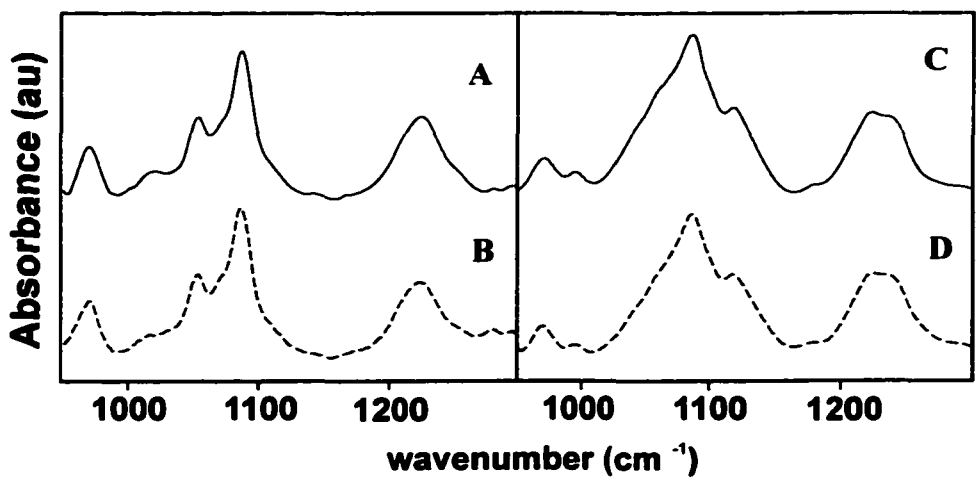

Figure 6. Trace a) FT-IR absorption spectrum of an aqueous DNA solution (2% w/w) measured using 5 micron pathlength and BaF_2 windows; trace c) FT-IR absorption spectrum of an aqueous RNA solution (2% w/w) measured using 5 micron pathlength and BaF_2 windows; trace b) FT-ATR spectrum of aqueous DNA solution (2% w/w) and trace d) FT-ATR spectrum of aqueous RNA solution (2% w/w) and trace. The spectra were not normalized.

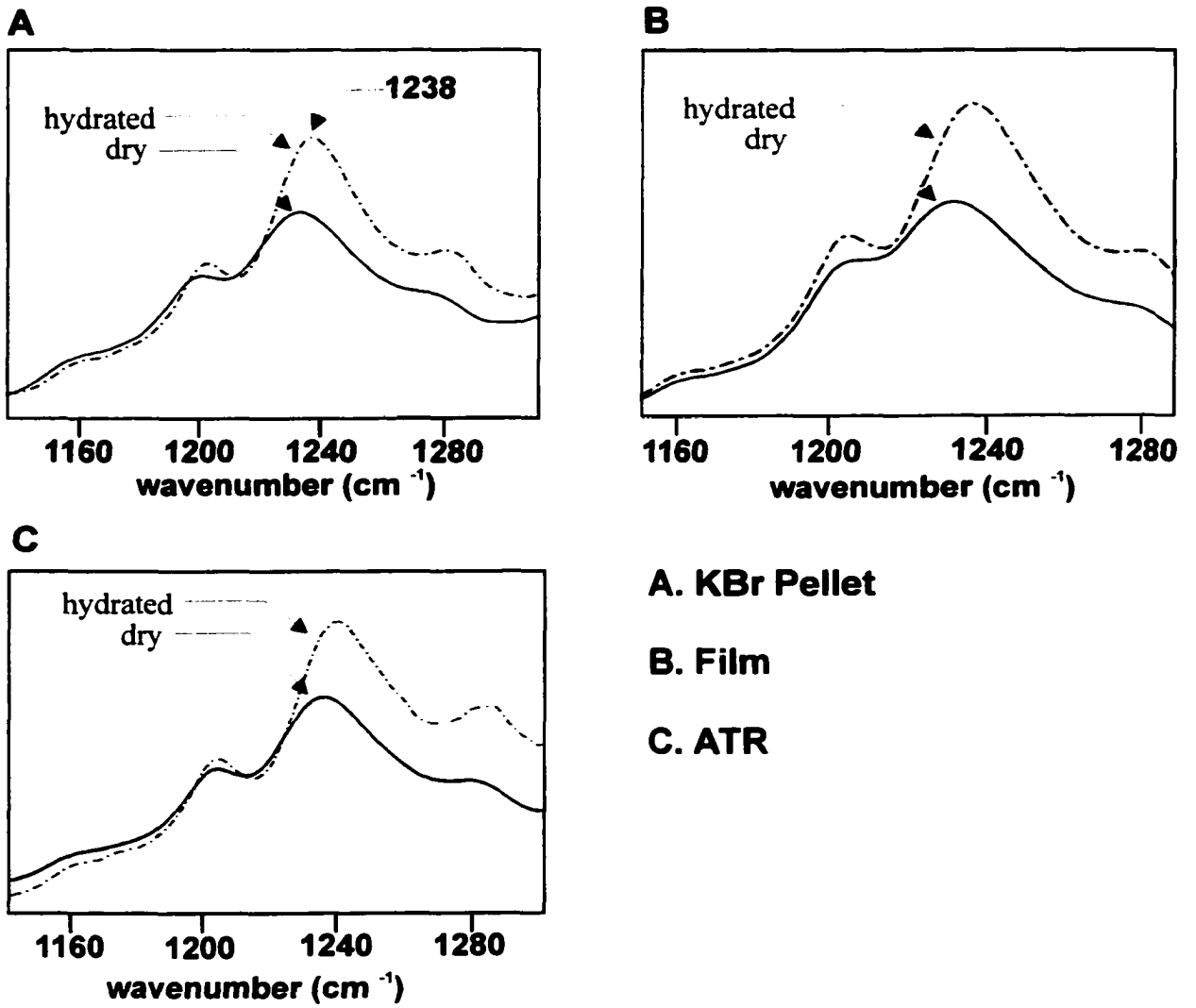

Figure 7. A) The spectra of hydrated and dry collagen from KBr pellet hydration study; B) the spectra of hydrated and dry collagen from film hydration studies and C) ATR spectra of collagen gel, hydrated and dry .

Summary

The hydration experiments with both KBr pellets and films clearly show a direct dependence of vibrational spectra of proteins, nucleic acids and phospholipids on the amount of bound water. The water that is present in a structure of a molecule is able to modulate the intensities and frequencies of a number of bands, and in addition may cause structural transition from one conformation to the other. For proteins, regardless of secondary structure, bound-water effects intensities of amide I, amide II and the shape of amide III band. The intensity increase by almost a factor of two for amide I vibration in most likely to be a consequence of the increase of dielectric in the close proximity of the polar C=O bond. The diminishing half-widths of amide I band and the change of curvature of amide III that accompany the increase in intensity are explain as structural modification that protein may undergo when amount of bound water in a molecule goes up. This slight conformational adjustment in a protein can be result from a fact that in dry polycrystalline protein a broader distribution of conformational angles ϕ and ψ exists, and in the hydrated state, on the other hand, the protein may assume a new structures with more narrowly defined conformational angles ϕ and ψ.

For DNA, RNA and phospholipids the increase in bound water effects mostly the vibrational modes of PO_2^- group. The intensity increase of ν_S PO_2^- and a frequency shifts of ν_{AS} PO_2^- are observed when these molecules are exposed to water vapor. The intensity increase may be of the same origin as

that observed for C=O mode in proteins. The presence of water in a vicinity of charged PO_2^- group increases the local dielectric and consequently the intensity of ν_S PO_2^-. The DNA molecules upon uptake of water transforms from A-form to a B-form. The structure of RNA and phospholipids are not effected by water, but water may well effect the geometry of the PO_2^- group. These conformational changes can explain the frequency shift of ν_{AS} PO_2^-, ranging from 2-12 cm^{-1}, observed for DNA,RNA and phospholipids.

For all cases examined, proteins with different secondary structural motifs, DNA , RNA and phospholipid, the variation in the amount of bound water effect most strongly the vibrational frequencies and intensities of highly polar and charge bearing functional groups. In addition, as stated before, this work demonstrates that infrared patterns observed for the main cellular components are directly affected by hydration state of a biological sample.

The research presented in this thesis has a direct application to the study of cells and tissues by infrared spectroscopy. First, it had answered the question that it was aimed to answer when this experimental work has started. "Why does in some cases the same sample of cells produces different spectra". This study demonstrates that a hydration state of a sample alone can be the cause of inconsistency in the measurements. Second, this research points out the importance of sample preparation procedures, and consequently will lead to the development of infrared sampling protocol for cells, tissues and biomolecules that is consistent and artifact free.

Bibliography

Introduction

1. Wong, P,T.; Wong, R,K.; Caputo, T,A.; Godwin,T,A.; Rigas, B. IR Spectroscopy of Exfoliated Human Cervical Cells; Evidence of Extensive Structural Changes During Carcinogenesis. *Proc. Natl.Acad.Sci.USA*. **1991,** 88,10988-10992.

2. Cohenford, M.; Rigas ,B. . Cytologically normal cells from neoplastic cervical samples display extensive structural abnormalities on IR spectroscopy: Implications for tumor biology. *Proc. Natl. Acad.Sce.USA*. **1998**, 95, 15327-15332.

3. Benedetti, E.; Bramanti, E.; Papineschi,F.; Rossi,I.;Benedetti,E. Determination of the Relative Amount of Nucleic Acids and Proteins in Leukemic and Normal Lymphocytes by Means of Fourier Transform Infrared Microspectroscopy (FT-IR-M). *Appl.Spectrosc.* **1997**, 51 (6),792-797.

3. Nauman,D.; Fijala,V.; Labischinski,H.; .Giesbrecht, P. The rapid differentiation and identification of pathogenic bacteria using FT-IR and multivariate statistical methods. *J.Mol. Struct.* **1988**, 174, 165-170.

4. Helm,D.; Labischinski,H.; Schallen, G.; Naumann, D. Classification and identification of bacteria by FT-IR spectroscopy. *J.Clin.Microbiol.* **1991**,137, 69-79.

5. Sockaland, S,G.; Bouhedja,W.; Pina, P.; Allouch, P.; Bloy,C.; M.Monfait,M. FT-IR Spectroscopy as an Emerging Method for Rapid Characterization of Microorganisms. *Cell.Mol. Biol.* **1998**, 44 (1), 261-269.

7. Ngo-Thi,N,A.; Kirschner,C.; Naumann,D.; FT-IR mircoscopy: a rapid method for classifying microorganisms. In *Spectroscopy of Biological Molecules: New Directions;* Greve, J.,Puppels G.J,. Otto, C.,Eds.; Kluwer Academic Publishers: Dordrecht (Netherlands),1999: pp.557-559.

8. Chiriboga,L.; Xie,P.; Yee,H.;Vigorita,V.; Zarou.D.; Zakim,D.; Diem,M. Infrared Spectroscopy of Human Tissue: I. Differentiation and Maturation of Epithelial Cells in the Human Cervix. *Biospectrosc,***1998**,4, 47–54.

9. Boydston-White,S.; Gopen,T.; Houser,S.; Bargonetti,J.; Diem,M. Infrared Spectroscopy of Human Tissue: V. Infrared spectroscopic studies of Myeloid Leukemia (ML-1) cells at different phases of the cell cycle. *Biospectrosc*, **1999**, **5**, 219-227.

10. Lasch, P.; Pacifico, A.; Chiriboga, L.; Diem, M. Infrared Microspectroscopy and Infrared Spectral Maps of Single Human Cells. *Nature*, submitted for publication 2001.

11. Diem, M.; Boydston-White, S.; Chiriboga, L.; Infrared spectroscopy of Cells and Tissues: Shining Light onto a Novel subject. *Appl.Spectrosc.***1999**, 53 (4),148A-161A.

Chapter 1

1. Wilson B.E; Decius,J,C; Cross, P.C. *Molecular Vibrations: The Theory of Infrared and Raman Vibrational Spectra.* McGraw-Hill: , New York, 1955.

2. Levine,Ira. *Molecular Spectroscopy.* John Wiley & Sons: New York, 1975.

3. Diem, Max. *Introduction to Modern Vibrational Spectroscopy.* John Wiley & Sons: New York, 1993.

4. Colthup,N,B;Daly,L,H; Wiberley,S,E. *Introduction to Infrared and Raman Spectroscopy.* 3rd Ed; Academic Press: New York,1990.

5. Foresman,J,B; Frish,E. *Exploring Chemistry with Electronic Structure Methods.* 2nd Ed; Gaussian, Inc: Pittsburgh, 1996.

6. Gaffey,M,L;Dobosh,P,A;Richardson,D,M. *Laboratory Exercises Using Hyperchem®.* Hypercube,Inc: Gainesville, Florida, 1998.

7. Griffiths, P,R; de Haseth, J,A. *Fourier Transform Infrared Spectroscopy*; Chemical Analysis; Vol 83. Jonh Wiley & Sons: New York,1986.

8. Smith,B,C. Fundamentals of Fourier Transform Infrared Spectroscopy. CRC Press: Boca Raton, Florida, 1995.

Chapter 2

1. Savitsky,A.; Golay,M,J,E. Smoothing and Differentiation of Data by Simplified Least Squares Procedures. *Anal.Chem* . **1964**, 36 (8), 1627-1639.

2. Mitchell, R. ; Harris, P,I.; Fallowfield,C. ; Keeling,D,J.; Chapman C. Fourier transform infrared spectroscopic studies on gastric H^+/K^+-ATPase. *Biochem. Biophys. Acta.* **1988**, 941, 31-38.

3. Miyazawa,T.; Shimanouchi ,T.; and Mizushima, S. Normal vibrations of N-methylacetamide. *J.Chem.Phys.* **1958**, 29,611-616.

4. Miyazawa,T. Characteristic Amide bands and conformations of polypeptides. In *Polyamino acids,Polypeptides and Proteins.* Stahmann, M, A.,Ed. University of Wisconsin Press: Madison, WI, 1962; pp 201-217.

5. Jakes,J.; Krimm S. Normal coordinate analysis of molecules with the amide group. *Spectrochim.Acta. Part A* .**1971**, 27,35-63.

6. Krimm,S.; Bandekar,J. Vibrational spectroscopy and conformation of peptides,polypeptides and proteins. *Adv.Protein.Chem.* **1986**,38,181-363.

7. Oboodi M.R.; Alva, C.; Diem,M. Solution-Phase Raman Studies of Ananyl Dipeptides and Various Isotopomers: A Reevaluation of Amide III Vibrational Assignment. *J.Phys.Chem.* **1984**,88,501-505.

8. Asher, S,A.; Lanoul, A.; Mix, G.; Boyden,M.; Karnoup,A.; Diem,M.; Schweitzer- Stenner,R. Dihedral Angle Dependence of the Amide III Vibration: A Uniquely Sensitive UV Resonance Raman Secondary Structural Probe. *J.Amer.Chem.Soc.*, submitted (2000).

9. Jackson, M.; Mantsch H,H. The use and misuse of FTIR Spectroscopy in the determination of protein structure. *Crit.Rev.Biochem.Mol.Biol.* 30 (2), **1995**,95-120.

10. Cantor,C,R.; Shimmel P,R. Absorption spectroscopy. *Biophysical Chemistry Part II: Techniques for the study of biological structure and fucntion.* W.H.Freeman and Company: New York,1980; pp 349-408.

11. Diem, M. Biophysical Applications of Vibrational Spectroscopy. *Introduction to Modern Vibrational Spectroscopy.* Jonh Wiley & Sons: New York, 1993; pp 204-225.

12. Silva, R.A.G.D.; Kubelka,J.; Bour, P.; Decatur.; Keiderling,T,A. Site-specific conformational determination in thermal unfolding studies of helical peptides using vibrational circular dichroism with isotopic substitution. *Proc.Natl. Acad.Science.* **2000**,97(15), 8318-8323.

13. Brauner, J.W., C.Dugan and R.Mendelsohn. ^{13}C Isotope Labeling of Hydrophobic Peptides. Origin of the Anomalous Intensity Distribution in the Infrared Amide I Spectral Region of β-Sheet Structures. *J.Amer.Chem.Soc.* **2000**, 122 (4), 677-683.

14. Brown, T.L.; Infrared Intensities and Molecular Structure. *Chem.Rev.* **1958**, 58, 581-609.

15. Halliday,D.; Resnick,R.; Walker,J. Electromagnetic Waves. *Fundamentals of Physics*. 4th Ed; John Wiley & Sons: New York, 1993; Vol 2, pp 988-1010.

16. Fujiyama,T:Crawford,B,Jr. Vibrational Intensities.XXI.Some Band Shapes and Intensities in Liquid Hexaflourobenzene. J.Phys.Chem. **1968**, 72, 2174-2181.

17. Han, W,G.; Jalkanen K,J,; Elstner, M.; Suhai,S. Theoretical Study of Aqueous N-Acetyl-L-alanine N'- Methylamide: Structures and Raman, VCD, and ROA Spectra. *J.Phys.Chem. B.* **1998**, 102, 2587- 2602.

Chapter 3

1. Pevsner, A. ; Diem, M. Infrared Spectroscopic Studies of Major Cellular Componets.Part I. The effect of Hydration on the Proteins. *Appl.Spectrosc.* **2001**, 55 (6), 788-793.

2. Dickerson, R,E. The DNA Helix and How It Is Read. *Sci.Amer.* **1983**,249 (6), 94 -111.

3. Dickerson, R,E.; Drew,H,R.; Conner, BN.; Wing,R,M.; Fratini, A,V.; Kopka, M,L. The Anatomy of A-,B-,and Z-DNA, *Science*, **1982**, 216 ,475-485.

4. Branden, C.; Tooze, J. DNA Structures. *Introduction to Protein Structure*" 2nd ed, Garland, New York,1998; pp212-126.

5. Saenger, W. *Principles of Nucleic Acid Structure*; Springer-Verlag, New York,1984.

6. Sutherland, G,B,B,M.; Tsobui, M . The infared spectrum and molecular configuration of sodium deoxyribonucleater. *Proc.Royal Soc.* **1957**, 239, 446-463.

7. Bradbury, E,M.; Price,W,C.; Wilkinson G,R . Infrared Studies of Molecular Configurations of DNA. *J. Mol. Biol.* **1961**, **3**,301-317.

8. Falk, M.; Hartman, K,A.; Lord, R,C. Hydration of Deoxyrobonucleic Acid.I.Gravimetric Study. *J.Amer.Chem.Soc.***1962**, 84, 3843-3846

9. Falk, M,; Hartman, K,A.; Lord, R,C Hydration of Deoxyrobonucleic Acid.II .An Infrared Study.*J.Amer.Chem.Soc.* **1963**, 85,387-993.

10. Falk,M.;Hartman, K,A.; Lord, R,C. Hydration of Deoxyrobonucleic Acid.III. A Spectroscopic Study of the Effect of Hydration on the Structure of Deoxyribonucleic Acids. *J.Amer.Chem.Soc.*, **1963**, 85, 391-394.

11. Hartman, K,A.; Lord, RC.; Thomas,G,J. Structural Studies. In *Physico-Chemical Properties of Nucleic Acids*" vol 2. Duchesne,J Ed; Academic Press; New York, 1973,Vol 2,pp2-89.

12. Parker, F,S. Nucleic Acids and Related Compounds . *Applications of Infrared, Raman, and Resonance Raman Spectroscopy in Biochemistry*; Plenum Press, New York, 1983; pp349-398.

13. Taillander, E.; Liquier, J.;Taboury, J,A. Infrared Spectral Studies of DNA Conformations. In *Advances in Infrared and Raman Spectroscopy*. vol 12. Clark, R.J.H. and Hester, R.E., Eds; John Wiley & Sons; New York, 1985.pp: 65-114.

Chapter 4

1. Pevsner, A.; Diem, M. Infrared Spectroscopic Studies of Major Cellular Components. Part.I.The effect of Hydration on the Spectra of Proteins. *Appl.Spectrosc.* **2001,** 55 (6),788 – 793.

2. Pevsner, A.; Diem, M. Infrared Spectroscopic Studies of Major Cellular Components.Part.II. The effect of Hydration on the Spectra of Nucleic Acids. *Appl.Spectrosc.* **2001,** 55(6), 1502-1511.

3. Sutherland, G,B,B,M.; Tsobui, M . The infared spectrum and molecular configuration of sodium deoxyribonucleater. *Proc.Royal Soc.* **1957**, 239, 446-463.

4. Bradbury, E,M.; Price,W,C.; Wilkinson G,R . Infrared Studies of Molecular Configurations of DNA. *J. Mol. Biol.* **1961**, **3**,301-317.

5. Falk, M,; Hartman, K,A.; Lord, R,C. Hydration of Deoxyrobonucleic Acid.II.An Infrared Study.*J.Amer.Chem.Soc.* **1963**, 85,387-993.

6. Parker, F,S. Model Membranes, Biomembranes, and Lipid Containing Systems. In *Applications of Infrared, Raman, and Resonance Raman Spectroscopy in Biochemistry* Plenum Press; New York, 1983; pp381-401.

7. Casal, H.;Matsch, H,H. Polymorphic Phase Behaivor of Phospholipid Membranes studied by Infrared Spectroscopy. *Biochim. Biophys.Acta.* **1984**, 779, 381-401.

Chapter 5

1. Harrick,N.J. *Internal Reflection Spectroscopy*.John Wiley & Sons, New York, 1967.

2. Heise, H,M; Marbach, R; Janatsch, G: Kruse-Jarres,G.D. Multivariate Determination of Glucose in Whole Blood by Attenuated Total reflection Infrared Spectroscopy. *Anal.Chem.*, **61**, 2009-2015 (1989).

3. Janatsch, G; Kruse-Jarres,J,D; Marbach,R; Heise,H,H . Multivariate Calibration Assay in Clinical Chemistry Using Attenuated Total Reflection Infrared Spectra of Human Blood Plasma. *Anal.Chem.*, **61**, 2016 (1989)

4. Heise,H,M; Marbach, R;Koschinski,T ;Gries, F,A. Multicomponent Assay for Blood Substrates in Human Plasma by Mid-Infrared Spectroscopy and its evaluation for Clinical Analysis. *Appl.Spectrosc.*, **48**(1), 85-95 (1994).